UNIVERSITY OF CALIFORNIA
RIVERSIDE

An Assessment of the Roles of the Neural Receptor IR40a in the Attraction of Flies, and an Attempt to Modulate IR40a in Mosquitos With the CRISPR/Cas9 System

A Thesis submitted in partial satisfaction
of the requirements for the degree of

Master of Science

in

Cell, Molecular, and Developmental Biology

by

Alden Teague Gaines

June 2017

Thesis Committee:
Dr. Anandasankar Ray, Chairperson
Dr. Jeffrey Bachant
Dr. Naoki Yamanaka

The Thesis of Alden Teague Gaines is approved:

_____

_____

_____

Committee Chairperson

University of California, Riverside

Acknowledgments

I would like to thank Dr. Anandasankar Ray and the Ray Lab: Tom Guda, Christi Ann Scott, Crystal Pontrello, Jadrian Oel Ejercito and Christine Pham. The Akbari, White, Dahanukar and Atkinson Labs at UCR have made my Master's research possible. With deepest gratitude to the Santa Barbara Scholarship Foundation for their funding and assistance.

Dedication

I cannot express my gratitude for the mentorship and support of Jason Knisley, Cliff Lamb-Rosa, Michael Black, Christy Strand, Pat Fidopiastis, Elena Keeling, Francis Villablanca, Megan Howard, Gita Kolluru, Jeffrey Bachant, Naoki Yamanaka, Martín García-Castro, Omar Akbari, Seema Tiwari-Woodruff, Patricia Springer, Frances Sladek, Howard Judelson, Morris Maduro, Daniel Terry and countless friends. Alan Cheng and David Benaron from Stanford and Jian Zuo from St. Jude Children's Research Hospital have been a source of inspiration to keep me going. I would not be here without the Ill, Fry and Gaines Families. I owe a debt to the House Clinic for saving my life. The Santa Barbara Scholarship Foundation, COSMOS, Genentech and the Santa Barbara Natural History Museum made it possible for me to reach this point and sparked my interest in science.

In fond memory of Robert Wiles.

Table of Contents

I. Introduction and Literature Review……Page 1

II. Chapter 1: The Role of IR40a in Humidity Sensation and Behaviors……Page 16

III. Chapter 2: The Application of the CRISPR/Cas9 System in *Aedes aegypti* to Target Ionotropic Receptor Genes……Page 30

IV. Conclusion……Page 46

V. References……Page 47

VI. Figures……Page 53

VII. Tables……Page 71

List of Tables

Table 1: Preference Index Values of 70%/70% Relative Humidity Gradient Behavioral Assays……Page 71

Table 2: Preference Index Values of 20%/70% Relative Humidity Gradient Behavioral Assays……Page 72

Table 3: Genomic Targets of CRISPR/Cas9 in *Aedes aegypti*……Page 73

Table 4: Primers Used for Diagnostic Restriction Digest……Page 74

Table 5: Data Summary of CRISPR/Cas9 of Ionotropic Receptor Genes in *Aedes aegypti*……Page 75

List of Figures

Figure 1: Phylogenetic Analysis and Alignment of IR25a……Page 53

Figure 2: Phylogenetic Analysis and Alignment of IR40a……Page 54

Figure 3: Sequence Confirmation of *IR40a(6)* and *IR40a(7)* Mutants……Page 55

Figure 4: Alignment of IR40a in Insect Species……Page 56

Figure 5: Analysis of *IR40a(6)* Mutant *Drosophila melanogaster*……Page 57

Figure 6: Analysis of *IR40a(7)* Mutant *Drosophila melanogaster*……Page 58

Figure 7: Illustration of Knecht et al. and Enjin et al.'s (2016) Results……Page 59

Figure 8: Knecht et al. and Enjin et al.'s (2016) Humidity Gradient Behavioral Assay Rigs……Page 60

Figure 9: Humidity Gradient Behavioral Assays Rigs……Page 61

Figure 10: Preference Index Results of Humidity Gradient Behavioral Assays in *Drosophila melanogaster*……Page 62

Figure 11: The CRISPR/Cas9 System and Breeding Scheme……Page 64

Figure 12: Egg Laying Chamber……Page 65

Figure 13: *Aedes aegypti* Egg Case Melanization and Microinjection Angle……Page 66

Figure 14: IR25a and IR40a Genetic Structures and sgRNA Cut Sites……Page 67

Figure 15: Diagnostic PCR Product and Cut Sites……Page 68

Figure 16: Diagnostic Restriction Digest……Page 69

Figure 17: Retrogen Sequencing Results……Page 70

Introduction

Many members of the Diptera Order are major disease carriers and others can cause agricultural destruction and thus can be considered among the most dangerous threats to humanity. The ability to sense environmental stimulus is central for these insects' feeding, reproduction and survival. Characterization of how these insects sense their environment needs more study. However, it is well worth the effort as endeavors to control wild populations by disrupting such insects' senses have been met with some success. Discovering how these insects sense their environment at the molecular level is essential in advancing the effort to control these dangerous pests. Two genes previously evidenced to be influential in insects' ability to detect and respond to sensory cues, IR40a and IR25a, seem to be fundamental in humidity sensation (Enjin et al., 2016; Knecth et al., 2016). However, these genes, while conserved and implicated in important sensory roles, are not fully understood. With recent breakthroughs in genetic editing, the creation of sensory deficient strains of transgenic insects has gained considerable attention since they could be used to curtail wild insect populations and serve as research models. Gaining greater insight into the sensory functions and mechanisms of these genes could have widespread applications, not just in pest management, but may also have uses in medicine or bioengineering. For example, if we find human homologues for these insects' sensory genes, we may identify genetic candidates that cause diseases that inhibit sensory functions. My work in the Anandasankar Ray Lab at University of California at Riverside (UCR) included testing the roles of sensory neuronal

receptors in flies and attempting to create sensory deficient IR25a and IR40a mutant mosquitoes through the new CRISPR/Cas9 system.

The ability to control sensory perception in wild populations of insects would be a massive boon to the survival and well-being of humanity. Mosquitoes transmit diseases to hundreds of millions of people every year, which is exemplified by the Yellow Fever Mosquito, *Aedes aegypti*, which spreads Dengue Fever, Zika Fever and several other diseases (Potter, 2014). Agricultural insect pests, many who belong to the family *Drosophilidae*, cause widespread food shortages around the world. Being able to counter insects' abilities to sense atmospheric humidity, egg-laying conditions, food, mates or predators would diminish these pest populations and reduce agricultural destruction and spread of disease. Of these sensory abilities, humidity sensation (hygrosensation) is insufficiently studied. In comparison, thermosensation has been well-characterized with established examples of temperature's influence of transcriptional regulation, signal transduction and the stability and conformation of proteins (Sengupta & Garrity 2013).

The development of a deeper understanding of how these insects perform hygrosensation has been the focus of much of this thesis. Additional experiments I performed at UCR included testing the CRISPR/Cas9 system in non-model organisms, primarily *A. aegypti,* with the hope of creating mutants with diminished hygrosensitivity or other sensory defects. The use of this powerful new approach to genome alteration

has been inadequately characterized in mosquitoes and needs greater refinement. As I have experimented with this system in relatively unexplored organisms, I am providing data that can be used to further understand the utility of this promising new tool and improve its implementation.

Hygrosensation research has slowly developed, lagging behind our understanding of many of the other senses and biological functions, despite it being one of the most crucial requirements for life (Knecth et al., 2016). Without the ability to sense water, animals would be unable to fulfill basic homeostatic functions. The inability to sense water sources leads not only to desiccation of the individual, but also can be lethal to eggs. The loss of the ability to sense humidity can also hinder these species' abilities to sense food sources and mates, which also rely on proximity to water. Conversely, excess humidity can lead to the hindrance of flight, homeostatic dysfunction and vulnerability to pathogens (Luz & Fargues, 1999).

Because of its importance, insect hygrosensation has been explored for decades, but only until the age of genetic manipulation have we seen breakthroughs promising tremendous utilitarian potential. Early researchers began by attempting to understand the anatomical and cellular structures that facilitate hygrosensation by focusing on the antenna, an ancient sensory structure prevalent in arthropods (Boxshall, 2004). In these publications, labs used electron microscopy and electrophysiology to provide evidence that the morphological structures on flies' antennae were at least partially responsible

for humidity sensation (Altner, Tichy & Altner, 1978; Foelix, Stocker & Steinbrecht, 1989). A later paper by Yao, Ignell and Carlson (2005) found two distinct types of coeloconic sensilla that demonstrated increases in electrophysical spike frequency with exposure to humid air and decreases in firing rates in response to dry air. Subsequent genetic studies used rudimentary single gene mutation techniques and surgical ablation of sensory organs to narrow down the anatomical structures and genes responsible for hygrosensation (Sayeed & Benzer, 1996). But now, we are capable of generating precisely gene edited mutants as well as conducting live calcium imaging, which has greatly enhanced neural molecular research (Knecth et al., 2016).

Relatively recently, a subfamily of Ionotropic Glutamate Receptors (iGluRs), called Ionotropic Receptors (IRs), have been demonstrated to play roles in thermosensation and hygrosensation (Knecth et al., 2016). These suspected descendants of iGluRs function through ligand-gated heteromeric complexes and are being demonstrated to provide complementary stimuli detection to Olfactory Receptors (ORs). ORs are quite divergent, having been shown to perform broad roles in odorant sensation, with species-specific profiles (Fuss & Ray, 2009; Abuin et al., 2011; Zhou et al., 2012). The IR subfamily is functionally distinct from many iGluRs. While iGluRs have been demonstrated to be involved in postsynaptic transmission of information, the IRs are being discovered to be involved in primary sensory roles (Abuin et al., 2011). Thus, learning more about the IR systems' functions provides an opportunity for novel investigation (Knecth et al., 2016). So far, some IRs have been implicated in several

odor-evoked responses, especially to acids and amines, making them distinct from normal ORs sensory stimuli (Yao et al., 2005; Abuin et al., 2011). However, in addition to IRs' ability to detect odorants, a subgroup of IRs observed in insect antennae have recently been found to detect heat and humidity (Benton, Vannice, Gomez-Diaz & Vosshall, 2009). According to Vosshall et al. (2009) and Rytz, Croset and Benton (2013), there are only ~16 antennal IRs, with some of the more basal ones (IR8a, IR21a, IR25a, IR40a, IR68a, IR76b and IR93a, for instance) drawing significant attention as they may represent fundamental evolutionary properties due to their substantial levels of conservation across Protosomia (Rytz et al., 2013).

IRs have a widespread presence among species, ranging from insects to mollusks. A growing body of evidence indicates that IRs evolved before ORs (Croset et al., 2010). Partial support for this hypothesis comes from the broad presence of IRs among Protostomia, whereas ORs are generally found in more recent evolutionary branches, like terrestrial insects (Croset et al., 2010). The two groups (IRs and ORs) seem to perform complementary roles in the classes of compounds they can detect (Abuin et al., 2011). This suggests that the IRs may have filled some of the most basic roles for the survival in aquatic ancestors, like the detection of water-soluble stimuli and environments with different osmolarities, leading to thermal and osmotic stability. On the other hand, the highly divergent ORs may have been a result of transitioning to a novel terrestrial environment with volatile stimuli (Missbach et al., 2014). The limited number of sensory candidate genes in *D. melanogaster's,* ~60 ORs and 66 IRs, compared

to ~1300 ORs in mice, makes *D. melanogaster* a good model to decipher some of the most fundamental sensory systems (Benton et al., 2009; Robertson, Warr & Carlson, 2003; Abuin et al., 2011).

The sacculus—a specialized structure on *D. melanogaster* antennae—has been firmly established to play roles associated with sensory functions and is a good model for study (Shanbhag, Singh & Singh, 1994). In this organ, poreless sensilla exist among other more conventional sensilla. So far, of the 16 antennal IRs, only five have been found to be expressed in the sacculus: IR8a, IR25a, IR40a, IR64a and IR93a (Rytz et al., 2013). Because a small number of IRs reside within the specialized sensory structure, it is reasonable to expect that these IRs hold relatively high biological value. IR8a and IR25a have been shown both to be common subunits for multiple antennal IR complexes, and to play central roles in the functionality of many other IRs. This, however, makes it difficult to pinpoint if they have any unique roles. IR40a, IR64a and IR93a have only recently been explored (Knecht et al., 2016). The fact that the sacculus resides in the antenna and contains poreless sensory sensilla makes it a promising place to search for stimuli detection mechanisms that sense signals that are not propagated via particulates (i.e. odors) (Rytz, et al., 2013). Changes in pressure or heat may be more likely stimuli for the sacculus' poreless-sensilla to detect, as particulates cannot penetrate the cuticular surface and reach the adjacent sensory cells. The arista—the other specialized structure on *D. melanogaster* antennae—is a feathery extension that contains, among various IRs, IR21a and IR25a and was demonstrated to also have

importance in humidity and temperature sensation (Sayeed & Benzer, 1996). However, a recent study indicated that the IRs in the sacculus and the IRs in the arista have different humidity related functions, with the former inducing thirst behaviors and the latter functioning in humidity gradient aversion behaviors (Ji & Zhu, 2015). The newly identified IR subfamily offers new avenues to investigate thermosensory and hygrosensitive receptors.

We know at least some of the sacculus IRs in *D. melanogaster* have roles in hygrosensation (Enjin et al., 2016). IR93a, for example, has been strongly linked to hygrosensation, but not as the sole hygrosensation-granting IR (Knecht et al., 2016). IR25a is a coreceptor found in the sacculus, arista and other sensory structures. It has also been proven to be a cofactor in humidity-related functions (Benton et al., 2009; Enjin et al., 2016). IR8a (the other cofactor) and IR64a have been shown to play roles in odor sensation (Rytz et al., 2013). This leaves the remaining IR, IR40a, as a key suspect for non-particulate sensory functions, including hygrosensation (Rytz et al., 2013). Mosquitoes do not have a structure analogous to the *D. melanogaster* sacculus. Thus, we require *D. melanogaster* to serve as a model for these disease-vector insects.

In the last few decades, the investigation into hygrosensitive neural receptors in *D. melanogaster* has diverged into at least two foci. Some labs have continued investigating humidity sensation within the antenna, particularly with a recent focus on IRs. However, other researchers, like Kristin Scott and Teiichi Tanimura, have

investigated hygrosensation in other anatomical structures like the labellum or proboscis, focusing on a different set of genes (Cameron et al., 2010; Inoshita & Tanimura, 2006). Both approaches have reported success in eliminating hygrosensitivity and humidity-related behaviors. The variety of results generated by these labs present an unclear picture of hygrosensation as a whole, thereby raising the possibility that redundant systems could exist.

Of recent interest to the Scott Lab is the gene *Pickpocket 28* (*PPK28*). Their 2010 *Nature* paper demonstrated that the PPK28 protein played a key role in detecting water in *D. melanogaster* and was involved in drinking behaviors in response to water detection. When labeled via a Yeast Transcriptional Activator-Upstream Activating Sequence-Green Fluorescent Protein system (Gal4-UAS-GFP), GFP was detected in gustatory sensory axons that project to a primary taste region, the subesophageal ganglion. The paper demonstrates that PPK28 was also expressed in taste bristles on the proboscis and, upon making *PPK28* null mutants, the researchers found type-1 labellar taste sensilla demonstrated loss of response to water stimulation and were capable of being rescued via reintroduction of *PPK28* (Cameron et al., 2010). While using Phenolyzer^{tm}, I came across the human disease Acral Peeling Skin Syndrome, which is caused by mutations in the Transglutaminase 5 (*TGM5)* gene (Cassidy et. al., 2005). What makes *PPK28*, *TGM5* and *Waterwitch* (a gene commonly implicated in hygrosensation) fascinating is that they all share a high level of similarity to *A. aegypti* IR genes (~70% amino acid sequence similarity to IR25a, IR40a, IR76b and IR93a) (Montell,

2008). This is approximately the degree of similarity seen between these IRs themselves. It is intriguing that so many potential redundant sensory structures and pathways seem to have developed and how the nullification of genes within one structure could cause the impotence of the other sensory mechanisms. It is clear that the field of hygrosensation could benefit from a thorough investigation of insect IRs.

The CRISPR/Cas9 system is an amazing new genetic tool for targeted genome manipulation. It offers the ability to make precise small insertions and deletions (INDELs) or insert/excise lengthy sequences in a relatively easy, fast, specific, cost-efficient manner with few off-target changes or the need to insert docking sites. This system is already being used to fight diseases, produce designer organisms, and even correct genetic predispositions (Wu et al., 2013; Reardon, 2015). However, the system has pros and cons that are more evident to those who directly use it, but are unknown to the public and general scientific community. An example of this is demonstrated by new reports showing Human Immunodeficiency Virus (HIV), which was heralded to be one of the first diseases to be eliminated by CRISPR, becoming resistant to CRISPR in mice studies (Callaway, 2016). This becomes an important consideration as there are two other competing gene editing systems, Zinc-Finger-Nuclease (ZFNs) and Transcription Activator-Like Effector Nucleases (TALENs). All of these (CRISPR/Cas9, TALENs and ZFNs) are vying to become the system-of-choice for precise genome editing. There are many unknown factors about the CRISPR/Cas9 system that need to be understood better. As we do more exploratory work with this system, we will learn how

to employ it throughout its phenomenal breadth of medical and technological applications.

My investigation has provided information about the efficacy of the CRISPR/Cas9 system in non-model organisms while attempting to create sensory deficient insects, and can help us to fine-tune the methodology of the system. Despite mosquitoes like *A. aegypti* being one of the deadliest animals in the world, only very recently have publications appeared using CRISPR/Cas9 in any species of mosquitoes. In order to address this, I attempted to induce INDELs in *A. aegypti* to create strains with mutant IR25a and IR40a. These mutants would allow for greater insight into the roles of these IRs while providing information of their functions in mosquitoes, instead of a *D. melanogaster* model. Furthermore, creating mutant mosquito strains with the CRISPR/Cas9 system could lead to the commercial production of species suitable for Sterile Insect Technique (SIT). SIT is the release of lab grown pest strains with defects in survival and reproductive abilities, and it has been used to eliminate wild pest populations (Krafsur & Novy, 1987; Carvalho et al., 2015). Released mutants compete for wild mates, pass defects to offspring and may be designed with genetic "detonators" to kill progeny under specific conditions. SIT has been very crude so far as it often uses radiation to sterilize adults in an inefficient process with "random" results that could have unforeseen consequences. However, using the precise gene editing of the CRISPR/Cas9 system to create INDELs or insert/excise constructs, the efficacy of this paradigm could be vastly improved. Gaining insight into employing the CRISPR/Cas9

system in non-model insect organisms is an exploration into the forefront of *in vivo* gene manipulation and could provide vast improvements to human quality of life.

The revolutionary CRISPR/Cas9's story began with Francisco Mojica's recognition that Clustered Regularly Interspaced Short Palindromic Repeats (CRISPR) existed in the genomes of very distantly related prokaryotes and his subsequent publications in the early 1990s (Lander, 2016). Barranguo et al. (2007) was the first paper to experimentally demonstrate the function of the combination of these CRISPR structures and *CAS* (CRISPR Associated) genes and empirically confirm that the system functioned as an adaptive immune system in prokaryotes against bacteriophages. The lab challenged wild-type *Streptococcus thermophilus* with bacteriophages and found that the resistant strains that arose had gained sequences with incredibly high homology to the bacteriophages within the spaces between the palindromic sections of the CRISPR regions. They tested *CAS* loss-of-function mutants and they found that the inactivation of *CAS* genes, particularly the gene that created the protein Cas9 (CRISPR Associated protein 9) caused the adaptive immunity system to become dysfunctional. From this work, we were introduced to the CRISPR/Cas9 system in which prokaryotes can integrate foreign genetic sequences and use them as guides to combat invaders.

Since these pioneers' publications, we have clarified that the Cas9 protein from *S. thermophilus* can use Single-Guide RNA (sgRNA) as a matching template sequence to direct the protein to a complementary genetic sequence and cut double-stranded DNA

(dsDNA). For this reason, the system is becoming a popular genome editing tool for precise genomic cuts. The final molecular requirement for the Cas9 protein is a Protospacer-Adjacent Motif (PAM) sequence to be directly adjacent to the sgRNAs target (Gasiunasa, Barrangoub, Horvath & Siksnys, 2012). *Streptococcus pyogenes'* Cas9 (SpCas9, hereafter referred to as Cas9) is the commonly used endonuclease Cas protein variant in research at the moment, and it necessitates a "NGG" motif for the PAM; it was the version of Cas protein that we used in our experiments. When using Cas9, the cut site occurs three base pairs upstream of the 5' end of the PAM sequence.

Once the CRISPR/Cas9 system induces a cut, mutations can then arise in two ways. The first is through Non-Homologous End Joining (NHEJ), which results in random INDELs at the cut site. The second, called Homology Directed Repair (HDR), can be used to insert or excise larger genetic sequences using the cell's innate repair mechanisms. This is performed by co-injecting a template sequence that has arms homologous to the regions adjacent to the cut sites to insert a cassette between the two CRISPR/Cas9 cut sites. Alternatively, it is possible to inject a template with homologous arms that lacks the sequence between the cuts, thereby stabilizing the cut chromosome and allowing the distant sequences to be joined by normal cell repair mechanisms, thus removing the region between the cuts. HDR has been observed to occur at a lower rate in experiments so far, as exemplified in Kistler, Vosshall, and Matthews' (2014) injection of *A. aegypti* targeting the *Waterwitch* gene, wherein 24.57% of the Generation Zero (G0) survivors contained INDELs that occurred though NHEJ, but only 0.71% of survivors of

this HDR attempt contained the desired insert. As long as some requirements are met, the CRISPR/Cas9 system can perform a variety of gene editing functions and has successfully been used in a growing number of species (Suzuki et al., 2016; Kistler et al., 2014).

The PAM sequence is on average expected to occur once every 17 base pairs throughout the *A. aegypti* genome, making it possible to target essentially any genomic loci of interest with the CRISPR/Cas9 system (Kistler et al., 2014). However, this can be somewhat locus-dependent because genomes demonstrate a nucleotide bias, with different rates of certain nucleotides appearing at varying distances from genes. This is important to keep in mind when we consider that there are common motifs necessary for transcriptional regulation with nucleotide biases. This bias can necessitate researchers to use guides that contain Single Nucleotide Polymorphisms (SNPs) or target Untranslated Regions (UTRs). The consequences of being forced to use such sgRNA are not fully known at this point in time and requires greater investigation. However, designer Cas proteins are rapidly being developed that can recognize different PAM sequences, and thus the specific enzyme a lab needs will likely be available soon. It is becoming apparent that different genes, guides and regions of the genome have vastly different success rates with the CRISPR/Cas9 system, even within the same labs utilizing the same procedures. There are discrepancies in the efficiency of different sgRNAs targeting sequences within and between genes as well as across the genome, ranging from 0—70^{+}% cutting success (Basu et al., 2015; Kistler et al., 2014). This is exemplified

in Kistler' et al. (2014), wherein six different genes were all subjected to simultaneous injections of three different sgRNA per gene. The efficacy rate among G0 survivors ranged from ~4—72% within the same gene and had substantially different success profiles between the six different genes. This paper speculated that such findings may be due to chromosomal architecture/epigenetics, but as of yet it is unknown why different genes seem more or less compliant with the CRISPR/Cas9 system. The utilization of CRISPR/Cas9 microinjections may decrease fertility, as seen in both Basu et al. (2015) and in my own experiments. The greater availability of the data regarding success rates with different combinations of genes, reagents, and procedural variations is allowing for meta-analysis that is key to deciphering trends that explain the different success rates (Wong, Liu & Wang, 2015). Some phages have even been found to contain CRISPR/Cas9 inhibitors which adds another variable to consider (Pawluk, Bondy-Denomy, Cheung, Maxwell & Davidson, 2014). Two of the most important factors for both specimen survival and DNA cutting success seems to be finding the right sgRNAs and fine-tuning the delivery of Cas9 (Basu et al., 2015). There is a growing number of considerations to be taken into account when using the CRISPR/Cas9 system, and websites like AddGene provide guides for dozens of alterations that can be used to optimize one's experimental plan, including suggested choices of Cas variants, delivery methods, cutting strategies and verification techniques ("Addgene: CRISPR/Cas9 Guide", 2017).

Being at the forefront of the new generation of genome-editing tools means encountering many hurdles. Particularly, expanding the CRISPR/Cas9 system to non-model organisms is made more difficult because only some species, like *D. melanogaster* or zebrafish, have GAL4/UAS strains that can selectively express Cas proteins. This makes the CRISPR/Cas9 system incredibly more reliable and sophisticated, capable of targeting specific tissues and time points while often providing non-lethal amounts of Cas9 in these traditional species. Non-model organisms instead require trial and error to find the proper delivery methods and concentrations of Cas9, sgRNAs and even repair mechanism inhibitors. The physical methodologies involved in CRISPR/Cas9 microinjections and the associated animal rearing required therein are both crucial to successfully implementing the system, and must be optimized for each species. Different biological timing, humidities, injection orientations, injection pressures, injection volumes, needle opening sizes, needle types, recovery periods, temperatures and varying components of animal husbandry all need to be fine-tuned. Despite these concerns, the CRISPR/Cas9 system houses incredible potential and ostensibly will be the gene therapy technique of choice for the foreseeable future. My experience with this system has helped to generate data to accelerate the use of this technique in mosquito and non-model fly species by performing the troubleshooting inherent to most pilot studies.

Chapter 1

Introduction:

Different models exist of how insects perform humidity sensation and their resultant behaviors. It has been shown that a structure located on *D. melanogaster* antenna, the sacculus, plays a major role in this insect's hygrosensation (Sayeed & Benzer, 1996; Liu et al., 2007). It has been demonstrated that IRs, including IR25a, IR40a and IR93a play key roles within this structure (Knecht et al., 2016; Enjin et al., 2016). My goal is to confirm and characterize the claims that IR40a is necessary for wild-type behaviors in response to humidity gradients. This effort begins with affirming the phylogenetic identities of these IRs (Figures 1 and 2) and continues with behavioral assays (Figures 6, 7, 8 and 9). Using behavioral assays, I hope to validate or discredit the claim of IRs roles in these processes and allow for improved direction in the effort to characterize hygrosensation and the functions of IRs. Tests on the *D. melanogaster* IR40a gene were performed not only with the hope of further understanding fruit flies, but with the future goal of characterizing harmful insects, like *A. aegypti,* so that those species can be controlled.

Two important papers were written in 2016 by Knecht et al. and Enjin et al. that specifically investigate the sacculus IRs for the roles they play in hygrosensation. Combined, their conclusions can be summarized with the following: IR40a plays a unique role in behavioral responses to environmental humidity, while IR25a and IR93a

play stronger roles in hygrosensation as well as thermosensation. Testing and confirming these papers were a significant part of my research, wherein I used *D. melanogaster* with different mutant alleles of IR40a in humidity gradient behavioral assays.

In Enjin's et al. (2016) experiments, IR40a and IR93a deficient mutants and controls were tested in a 20/70% Relative Humidity (RH) gradient two-choice assay. This experiment utilized a humidity gradient that was generated with supersaturated solutions in multiwell plates with a polyester mesh cover. Flies could then migrate to their preferred side of the humidity gradient. Their side preference was manually scored and calculated as a Humid Preference Index (PI) on a scale from $^{-}$1 to 1, preference for the dry or humid side respectively. Knecht et al. (2016) used similar testing setups and employed a Dry Preference Index which simply inverts the meaning of the $^{-}$1 to 1 scale, with a more positive value indicating preference for the dry option. Combining the studies of Enjin et al. and Knecht et al. (2016), it can be reasonably assumed that *D. melanogaster*'s optimal humidity preference is ~70% humidity. Knocking down IR40a using a RNA Interference (RNAi) UAS-Gal4 system caused a reversal of the wild-type preference for 70% RH side and the flies instead choose the 20% RH side (Enjin et al., 2016). However, the phenotype was highly variable with a median PI of approximately $^{-}$0.4, with large Standard Error of the Mean (SEM) bars (~0.6). The complete reversal of, instead of a decrease in, humidity response behavior may be considered odd since this and previously cited papers show evidence of compensatory hygrosensation pathways.

Not only are these causes for concern, but the UAS and GAL-4 controls in this assay provide greatly differing results from each other, with medians differing by ~0.4 PI. Large quartile boxes, (~0.6 PI) on each arm, and data ranges from 1–-1 persist throughout much of Enjin's behavioral tests. Generally, when data sets range from the extremes of the boundaries, large data sets are required for valid conclusions. It is also odd that the Enjin et al. (2016) paper represents their data inconsistently with median bars in their behavioral tests instead of averages, though they claim to use averages during the statistical tests which they do not provide. However, the Enjin et al. (2016) paper uses means while illustrating the results of their thermosensation experiments in the same figure. In contrast, the data is presented using averages instead of medians in both the behavioral and calcium imaging humidity tests of IR40a and IR93a in Knecht et al. (2016).

In both the Enjin et al. and the Knechts' et al. (2016) papers, PIs in humidity behavioral assays have large quartiles, data ranges, SEM and Standard Deviation (SD) bars. In graphs provided by Knecht et al. (2016), there appears to be a prominent overlap of SD and SEM bars for *IR76b* as well as multiple *IR40a* mutants compared to the wild-type in their testing. In a 20/70% RH assay two choice assay, Enjin et al. (2016), show a PI of ~1.0 by the four-hour time point towards the expected humidity preference side, indicating that every fly in the experiment went to the 70% RH side. In my tests, I was able to achieve a positive preference index of 0.55 PI by the same final time point with ostensibly similar testing conditions (Figure 10A and 10B).

The Knecht et al. and Enjin et al. (2016) papers use calcium imaging of the neurons in the sacculus that contain the IRs of interest to bolster their suspicions that some of these IRs may be behind hygrosensation. Enjin et al. (2016) uses GFP labeling to confirm that IR25a and IR40a containing neurons both project to special glomeruli termed the "Arm" and "Column." This is similar to Abuin et al. (2011), which found the similar IR40a containing neuronal projections to the Arm and Column. Enjin et al. (2016) calcium imaged both IR25a, and IR93a and found activation in response to dry air, but not to humid air, in the Arm. In both cases, neither caused a response in the Column. However, when testing IR40a, they found responses in the form of increases and decreases in fluorescence when subjected to dry and humid air respectively. This is at odds with Knecht et al. (2016), whereupon performing the same calcium imaging tests with IR40a and IR93a mutants and rescues, they found significant responses in both IRs towards moist and dry air. The conflicting results of these papers demonstrate a greater need to investigate the roles of sacculus IRs in hygrosensation.

In testing *D. melanogaster* hygrosensativity behavior, I incorporated techniques from past studies in a manner which resulted in a data distribution with small error bars (Figures 7, 8, 9 and 10), while replicating the overall behavioral trends. This is an important confirmation to have in the recent and controversial field of discovering the roles of IRs. In my research, I also used the Odorant Receptor *OR83b(2)* mutant to help demonstrate that there were no olfactory confounding factors (Figure 10B). Additionally, only male subjects were used to avoid sexual attraction cues and I used

four one-hour time points, as used in the Enjin et al. (2016) paper. Furthermore, each time I ran the assay, I tested two repeats of each IR40a mutant strains, (*IR40a(6)* and *IR40a(7)* (Figure 3, 4, 5 and 6), and wild-type strain at the same time to avoid variation due to environmental and/or circadian factors. I used alternating orientation of the plates in my trials as well as using a leveler to avoid a bias due to subtle incline. Plates were checked with a laser thermometer to be ~22° Celsius on both sides before trials began to avoid variability due to temperature. New netting and multiwell-plates were used in each trial. A smaller age range of flies was used to avoid possible confounding factors due to differing developmental periods. Rather than RNAi or a UAS-GAL4 system, the two mutant IR40a fly strains were CRISPR generated. These mutants consisted of a single amino acid deletion (*IR40a(6)*) as well as a true frameshift null (*IR40a(7)*) (Figures 3, 4, 5 and 6). My work allows for a broader understanding and confirmation of the role of IR40a in humidity sensation and/or response.

Materials and Methods:

Humidity Gradient Preference Behavioral Assay

Methodology based on the Enjin et al. (2016), and Knecht et al. (2016), papers was used to detect behavioral preferences in *D. melanogaster* in response to humidity gradients. CRISPR generated mutants of IR40a (*IR40a(6)* and *IR40a(7),* both made by Sarah Perry of the Ray Lab) and an *Orco*$^{-}$ mutant (*OR83b(2)*, obtained from the Ray Lab), were used in conjunction with wild-type W118 Canton-S flies for these experiments. The

IR40a(6) and *IR40a(7)* sequences were confirmed by Retrogen Inc. sequencing (Figure 3). TMHMM 2.0 (Center for Biological Research, 2017) software predicts *IR40a(6)* to have an amino acid deletion that ostensibly does not interfere with the protein's functional domains and *IR40a(7)* to have massive loss in functional domains due to a five-nucleotide deletion at the 116th base pair position (Figure 5 and 6). Flies were raised at 25° Celsius using standard cornmeal-agar food. The day before the experiment, CO_2 was used to briefly anesthetize and separate 10–12 male *D. melanogaster* into vials containing standard cornmeal-agar food. The following day, these 6–8 day post-eclosion flies were transferred to an empty vial and allowed to starve for 30 minutes to an hour before the assay.

Supersaturated solutions of NaCl (70% RH) and LiCl (20% RH) (Sigma# 746398 and 746460, respectively), dissolved in deionized water (diH20), were used to establish humidity gradients. Supersaturated solutions can be made by increasing a solvent's temperature, allowing more solute to be dissolved in liquid than is typical at lower temperature. The temperatures to dissolve specific masses of salts to create supersaturated solutions and the relative humidity they produce depends on the salts used and has been well-documented (Wexler & Hasegawa, 1954). These solutions were heated until the excess solids were fully dissolved and then allowed to cool undisrupted in gasket sealed glass containers. For proof of concept, supersaturated solutions of each salt were made, tested with a humidity sensor and found to be +/- 3% RH from expected values. This reagent mix recipe was used for the ensuing tests. Before adding each trial's

specimen, the solutions and containers were checked with a laser thermometer to confirm they were at ambient room temperature (22° Celsius). These solutions were then portioned to the left and/or right half of a new Costar 3513 12-well cell culture plate (Catalog# UX-01959-06) using a random number generator (Figure 9). These plates were placed on a white paper background within a white-paper-lined-cardboard barrier, using no adhesives. Unused polyester mosquito netting (Catalog# 7250A) with ~1 mm^3 holes was placed on the plates to ensure no contact with the solutions. The plates were checked with a level to ensure there is was no elevation disparity. Pipette-tip box lids were used to cover the plates after the flies were placed onto the center of the plates, following a very brief cold-anesthetization. Plates were sealed with parafilm, being careful to avoid disturbing the contents. The lids and the leveler were cleaned with 70% ethanol before each trial and allowed ample time to dry. A four-hour period was then recorded on camera, with the lights on inside a closed room, at ~40–50% RH and an average lab room temperature of ~22° Celsius.

Two plates of each of the three stocks were generally tested at the same time for each assay run and the tests were run at approximately 12 P.M., 4 P.M. or 8 P.M.. Between each run, the orientation of the supersaturated solutions was reversed to ensure one side was not unfairly subjected to an unknown stimulus. When testing the NaCl/NaCl 70/70% RH control, sides were designated as NaCl(A) and NaCl(B) to ensure proper rotation. At the end of the run, plates were visually checked to ensure they contained the proper supersaturated solutions using crystal structure, and flies were

manually counted using the video recordings. Dead flies and flies touching the midline were not counted.

Preference Index for Moist Side Preference was calculated as: PI = (Number of flies on more moist side minus the number of flies on more dry side)/total number of flies.

Results:

Genetic analysis of IR25a, IR40a, *IR40a(6)* and *IR40a(7)*

The primary genes of interest in my immediate research were IR40a and IR25a (Figures 1 and 2). With the goal of translating the investigation of *D. melanogaster* IRs to those of *A. aegypti* and other species, the amino acid sequences of *A. aegypti* IR40a and IR25a were compared to *D. melanogaster,* humans, house mice, *Caenorhabditis elegans*, Norway lobster (*Nephrops norvegicus)*, spotted-wing drosophila (*Drosophila suzukii)* and the malaria transmitting mosquito *Anopheles gambiae*. The use of the National Library of Medicine's alignment and search program, BLASTP, of these genes' amino acid sequences, as predicted by VectorBase, demonstrated IR25a to be extremely conserved at the protein level among a broad range of species, especially insects (Figure 1). On the other hand, IR40a demonstrates conservation only within the Class Insecta (Figure 2 and 4). Figure 3 and 4 illustrate that IR40a is somewhat conserved among insects, and that the region where the INDELs were induced in the test mutant strains was substantially conserved. Figures 3, 4 and 5 demonstrate that the Ray Lab's stock *IR40a(6)* mutant

contains a single amino acid deletion that is absent from wild-type *D. melanogaster* in a region highly conserved among insects. Figure 5 demonstrates that the change in the *IR40a(6)* mutant does not change functional regions of IR40a predicted by the Center for Biological Sequence Analysis. Figures 3, 4 and 7 demonstrate that the Ray Lab's stock *IR40a(7)* mutant contains a five-nucleotide deletion, compared to wild-type *D. melanogaster*, in a region highly conserved among insects. Figure 6 demonstrates that the change in the *IR40a(7)* mutant eliminates the functional features of IR40a predicted by the Center for Biological Sequence Analysis. Genetic analysis shows that IR40a and IR25a have a considerable degree of conservation, in insects and more broadly in Protostomia respectively (but less so with IR40a), that makes them viable candidates to study with the goal of translating that knowledge towards other species for utilitarian purposes (Figures 1, 2 and 4). Interestingly, the arthropod *N. norvegicus* of the Crustacea Subphylum did not show homologous genes to IR40a nor IR25a using the National Institute of Health genome browsers. It is possible that the lack of detected homologous genes is due to incomplete genomes of the Crustacea and Chelicerata groups of arthropods (Gan, Tan, Gan, Lee & Austin, 2015).

Humidity Gradient Behavioral Assay of *D. melanogaster*

The two-choice assay using humidity gradients is an established method to infer sensation or response of species to humidity stimuli. The use of this assay helped give context to and reinforce the results of the two 2016 publications, Enjin et al. and Knecht

et al., on the abilities of *D. melanogaster* to detect and respond to humidity using IR function. My raw data and graphical representations can be seen in Tables 1 and 2 and Figure 10 respectively. Figure 7 summarizes the results of the Knecht et al. (2016) paper's 67/96% RH and 89/96% RH behavioral assays (in red) and the Enjin et al. (2016), paper's 20/70% RH experiments (in green). The width of the arrows indicates the degree to which mutations in the specified genes were found to affect behavioral preference. Figure 8 shows the behavioral assay chambers we used based loosely on the assay chambers used by Knecht et al. (2016), (on the left) and the chambers used by Enjin et al. (2016), (on the right). Figure 9 shows examples of two plates used in my assays. Figure 9A is a closeup of two plates. 9B is an image of the whole rig (white-paper lined, open-top box around the assay is not shown). Figure 10 graphically illustrates the PI results of my humidity gradient assays using NaCl/NaCl (70/70% RH gradient) and LiCl/NaCl (20/70% RH gradient) with *D. melanogaster*. These specimen were shown to display a preference towards a 70% RH compared to a 20% RH option, matching previous observations. The *OR83b(2)* mutant results indicate that this preference is not due to odor stimuli. The *IR40a(6)* results show that the flies still have the preference for the 70% RH option, but it may be to a lower degree than wild-type as the *IR40a(6)* mutant's mean PI is less than half that of the wild-type and *OR83b(2)* strains. The *IR40a(7)* displayed a deficiency in response to humidity gradients, matching the conclusions of the Knecht et al. and Enjin et al. (2016) publications.

Discussion:

From the above, we can see that IR40a is a relatively conserved gene within Class Insecta and that my experiment corroborated the results seen in the Enjin et al. and Knecht et al. (2016), papers but to different degrees. In a 20/70% RH gradient, my IR40a null mutant (*IR40a(7))* displayed a preference that was not statistically different than when it was tested in a 70/70% RH control condition (Two-Tailed T-Test P-value of 0.81) (Cumming, Fidler & Vaux 2007). By the fourth hour of the assay, the mean PI of my *IR40a(7)* mutant in the 20/70% RH assay was 0.14, while the PI in the 70/70% RH assay was $^{-}$0.28. The 20/70% RH assay result is quite different from the fourth hour PIs of the wild-type (0.55) and the *OR83b2* (0.67) controls (Figure 10). The lack of clearer results could be caused by compensatory pathways, or subtle differences in assay design or genetic background. However, my work does demonstrate IR40a in *D. melanogaster* was necessary for wild-type detection and avoidance behavior in a "too dry" environment.

Of note, my wild-type W118 and mutant IR40a mutant strains failed to display as decisive of a preference for the 70% humidity condition as seen in either Knecht et al. (2016) or Enjin et al. (2016). These papers showed that their controls were uniformly on the 70% RH side by the end of the assays and that their IR40a mutants demonstrated a massive decrease in their ability to respond to a humidity gradient. Only my *OR83b*

mutant had comparable results, but as Enjin et al. (2016) only provides the median values, it is hard to confirm this.

As mentioned previously, my *IR40a(6)* mutant was predicted to contain a silent mutation. Comparing the data of the *IR40a(6)* strain in the 70/70 RH% control and 20/70% RH test setups using an Unpaired Two-Tail T-Test resulted in a P-Value of 0.03, which by conventional criteria means that there was statistical difference in the flies' behaviors. This supports the premise that the mutation in *IR40a(6)* was not sufficient to knock out humidity-related behaviors. This is further supported when comparing the results of the 20/70% RH conditions of W118 and *IR40a(6)*, wherein a P-Value of 0.3 was calculated, meaning the wild-type and the mutant IR40a(6) strain demonstrated no statistically different abilities to respond to this humidity gradient. Of note though, a similar comparison of W118 and *IR40a(6)*s' data from what should be the control 70/70% RH assay resulted in a P-Value of 0.09, a low P-Value, but technically not one that clearly demonstrates significance. In comparison, an Unpaired Two-Tail T-Test of the results from the *IR40a(7)* frameshift mutant in the 70/70% control and 20/70% test conditions resulted in a P-Value of 0.8, indicating a loss in the mutant's ability to discern or respond to a humidity gradient. This key result supports the idea that IR40a is necessary for proper hygrosensation behaviors.

Figure 10 illustrates that my results were similar to those of the Knecht et al. and Enjin et al. (2016) papers and supports the conclusions of prior publications regarding

IRs; my research reinforces the idea that IR40a provides a role in hygrosensation in *D. melanogaster.* IR40a is predicted to be conserved among many of the most dangerous disease vector mosquitoes (*A. gambiae*, *Culex quinquefasciatus*, *Aedes albopictus*, and *Anopheles sinensis*), particularly in the region of the IR40a INDELs used in this study and conserved between *Diptera* as a whole (Figures 2 and 4). Because of this, the translation of our knowledge of IR40a from *D. melanogaster* to *A. aegypti* or the invasive *D. suzukii* (83% and 55% protein identity conservation respectively) (Figure 2) should create a better foundation to combat these pests.

Examining my experimentation with *D. melanogaster* IR40a mutants, I have come to a few conclusions. I suggest replicating this experiment with a larger data set in order to reach more definitive data. I would also suggest repeating the experiment only using females, as perhaps their egg-laying capacity could alter their ideal humidity-seeking behaviors. The unexpected results of missing alignments of *N*. *norvegicus* for IR40a and IR25a, as well as the presence of a substantial degree of alignment amongst *TGM5*, *Waterwitch*, *nanchang* and the IRs investigated in this paper, may warrant future investigation. Knockout combinations of IR8a, IR25a, IR40a, IR64b, IR93a, *Nanchung*, *PPK28*, *TGM5* as well as *Waterwitch*, should be tested to provide a better picture of hygrosensory pathways and structures. Additionally, these aforementioned genes should be compared using bioinformatic technology to see if there are common features behind these suspected hygrosensation genes. Likewise, the results of the humidity behavioral assay of the *IR40a(6)* mutant in comparison to the controls should

be kept in mind if future research using this strain is performed. By identifying hygrosensation genes and creating strains with mutations in these genes, we could launch an offensive opposition and gain quality of life benefits for the human species.

Chapter 2

Introduction:

I have been utilizing the CRISPR/Cas9 system in an attempt to create *A. aegypti* lineages with mutant IR genes, specifically IR40a and IR25a. This research can contribute to learning about the efficacy of the CRISPR/Cas9 system in this non-model parasite as a whole. Only very recently have any studies been published testing this gene editing technique in mosquitoes, generally *Anopheles* species, and these have been met with varying successes (Hammond et al., 2016; Gantz et al., 2015). While *D. melanogaster* has been optimized to work with the CRISPR/Cas9 system by the establishment of GAl4-UAS strains, allowing the targeted expression of Cas9 and/or sgRNAs, the creation of CRISPR/Cas9 mutant strains in mosquitoes is currently still a laborious process. Despite this, I attempted to create mutant IR lineages in *A. aegypti* which could serve as research models or be employed to control wild populations.

My investigation of the CRISPR/Cas9 system also included the analysis of a variety of genes that could be targets for future gene editing research in Diptera. This involved using a variety of CRISPR/Cas9 simulation softwares and detailed culling of genome databases (Montague, Cruz, Gagnon, Church & Valen, 2014). This research was recorded and may direct future breakthroughs by providing a stronger starting point and by diverting lab funds from genes that are, at this point, not readily compatible with CRISPR/Cas9 into more suitable areas.

As both *A. aegypti*'s range and the corresponding threat of viral outbreak expands throughout the United States, it is more crucial than ever to characterize this disease vector, assess its weaknesses and use new tools to exploit these weaknesses (CDC, 2017). In line with former Brazilian President Dilma Rousseff's declaration that we must "wage war on [...] *Aedes aegypti*," it is imperative that we assess the potential of the CRISPR/Cas9 technology in this fight (Reuters, 2017). The example of how the parasitic Screwworm (*Cochliomyia hominivorax*) was eliminated from the southern portion of the United States of America by releasing genetically manipulated males as a form of SIT has made it abundantly clear that infiltrating wild *A. aegypti* populations with genetically modified mosquitoes could be an excellent method to slow or even reverse that species' advance (Novy et al., 1987).

Instead of crudely using irradiation to make sterile males, as we did to eradicate the Screwworm, we can now employ the surgical precision of the CRISPR/Cas9 system to effectively eliminate current and future threats by way of disseminating genetically manipulated insects into wild populations. This technique could lead to more efficient SIT, and the company Oxitec has had exemplary success in the release of transgenic mosquitoes to reduce local populations. Using a system termed RIDL (Release of Insects carrying a Dominant Lethal gene), they were able to decrease wild populations in field trials by as much as ~95% over the course of a year (Carvalho et al., 2015). Instead of relying on irradiation, which creates mutant males less fit to compete with wild males, they instead raised transgenic mosquitoes that produced a protein that inhibits

transcriptional regulation and kills the individual (Harris et al., 2012). While they are being raised in the lab, this mechanism is inhibited using the drug Tetracycline. When released, the progeny that the mutants have with wild females are not exposed to the drug, and the offspring thus die. In line with these efforts, the data that I generated using the CRISPR/Cas9 system in *A. aegypti*, could be used to create hygrosensitivity deficient GMO mosquitoes that could function to combat wild disease carrying vectors.

Many of the publications of the use the CRISPR/Cas9 system in mosquitoes so far have sought to knock out or insert either fluorescent reporters, or other visible reporter genes in transgenic mosquitoes (Basu et al., 2015; Gantz et al., 2015) and have had some interesting results. Kistler, Vosshall and Matthews (2014) had varied success performing NHEJ with the CRISPR/Cas9 system across six genes simultaneously using three sgRNA per gene. However, they found one gene resistant to mutagenesis despite using six different sgRNA to attempt to cut the gene. They also found that two of four insertion sites where they attempted to induce HDR insertions of fluorescent markers failed to successfully integrate the cassette. Likewise, Basu et al. and Gantz et al. (2015) both found some sgRNA were unable to induce INDELs although they used large sample sizes. This indicates that there are still variables which we need to understand.

Dong et al. (2015) submitted the first report detailing the use of the CRISPR/Cas9 system in *A. aegypti*; however they noticed a lower efficacy than in established model organisms like *Drosophila.* Kistler et al. (2014) subsequently submitted, but was first to

publish, the first use of the CRISPR/Cas9 system in *A. aegypti*. These two papers were landmark breakthroughs in the effort to control this dangerous pest through this new genetic editing tool. Both papers explored the efficacy of delivery systems of Cas9/sgRNAs and the activity of different sgRNAs; moreover, they were able to successfully confirm the transmission of gene editing from G0 to G1 offspring.

By targeting a cassette containing a fluorescent marker, Dong et al. (2015) was able to create INDELs of varying lengths that disrupted the marker phenotype. They employed simultaneous injections of two sgRNA that targeted regions 431 base pairs apart from each other in the ECFP gene but found only one guide was able to produce cuts. Survival rates varied from 4.5–14% when using plasmids containing the Cas9 and sgRNA instructions and 11.7% when using RNA transcript versions for the injections. None of their plasmid-based attempts were able to pass on their INDELs from G0 to G1, but the free transcript attempt was successful. This paper grouped their RNA injected G0 survivors into 23 pools of 5–20, and of these, four produced G1 knockout individuals. Using this methodology and a few assumptions, they predicted a 5.5% knockout efficiency when using functional transcripts of sgRNA and Cas9.

Kistler et al. (2014) both targeted genes for NHEJ and used constructs to insert Enhanced Green Fluorescent Protein (EGFP) or *Discosoma* Red Fluorescent Protein (dsRED) fluorescent through HDR. Six different genes were targeted for NHEJ, and each with three different sgRNA localizing the Cas9 to different regions which resulted in ~0–

70% G0 mutation rates. The publication found one gene to be resistant to the system despite the use of six different sgRNA guides. They found no success using plasmid Cas9, so they switched to mRNA and protein Cas9, both of which showed success with the protein Cas9 proving superior in this instance with 5–10 times greater efficacy. It seems clear that even targeting the same genes in *A. aegypti* can result in different rates of survival and establishment of transgenic lineages when methodology is slightly altered.

Likewise, Basu et al. (2015) demonstrated variability in success rates of NHEJ and HDR when methodological variations or different sgRNAs were used with the CRISPR/Cas9 system in *A. aegypti*. While attempting to perform HDR, after screening ~91,000 embryos, they found only a success rate of <0.3–2.3% G1 transformation. This lab then suppressed the production of a protein involved in the end-joining response, Ku70, while attempting to insert a fluorescent gene cassette via HDR. They were able to both achieve gene insertion frequencies at rates comparable to traditional transposon or Phi-C31 integration methods, and create two lineages out of 1880 injected embryos. This method theoretically reduced NHEJ frequency and thus increased the odds of HDR occurrence, allowing precise insertion or excision of genetic sequences (Figure 13). This indicates that specimen that have temporarily reduced capacity to perform either NHDJ or HDR via RNAi interference can improve the success rate of one molecular function at the expense of the other (Basu et al., 2015). This interference must be temporary as permanently inhibiting molecular repair machinery can be lethal to the specimen.

Testing 40 sgRNAs across five different parts of the genome, Basu et al. (2015) identified variation among the effectiveness of guide RNAs (10–70% effectiveness in G0 transformation) and then used the most optimal guides to further increase the rates of germline transformation to 24–90%. This is in contrast with their attempts using the traditional TALEN reagent, which failed to produce a transgenic line. This clearly shows optimization techniques are advised when using the CRISPR/Cas9 system, but that the system may still be the superior gene editing technology.

Cas9 is probably the most fickle, sensitive and hazardous component of the system since normal microinjections cannot be exactly targeted to specific tissues. An example that highlights the importance of optimizing the CRISPR/Cas9 system is that increasing concentrations of Cas9 (1,200 ng/µL) and sgRNA (982 ng/µL) provided tremendously more survival and transformants in the Asian Swallowtail *Papilio xuthus* than when the lab used 300 ng/µL and 150 ng/µL respectively and observed no transformed individuals (Wang et al., 2015). Conversely, Kistler et al. (2014), claims that much lower Cas9 concentration (and further reductions from 500 ng/µL to 400 ng/µL) and relatively low sgRNA concentrations (from 40 ng/µL to 160 ng/µL) in *A. aegypti* were optimal for survival and transformation. The data I generated could help narrow down the optimal Cas9 concentration needed to create mutant *A. aegypti*.

By attempting to produce and characterize IR mutant mosquitoes using a cutting-edge technique, I am participating in understanding the behavior of one of the

most dangerous disease carrying vectors in the world. To that end, I used the CRISPR/Cas9 system to target IR40a and IR25a in *A. aegypti* using a single sgRNA per gene. These sgRNA contained a 23 complementary nucleotide sequence (including the PAM site) and were generated by Maria Irigoyen, a former member of the Anupama Dahanukar Lab at UCR (Table 3) (Figures 11 and 16). The second exon in IR25a was targeted: this sequence contained a silent SNP variant, AX-93248676, seven nucleotides downstream of its GGG PAM site that did not match the RNA guide. The IR40a cut site was designed to be 28 base pairs downstream of the ATG start site and utilized a GGT PAM sequence. Injecting Cas9 and sgRNA physically disrupts the cell and its developmental factors, which have substantial adverse effects on the health and fitness of the specimen. This can be exemplified where, even in well-respected hands, merely injecting diH20 as a control for a CRISPR/Cas9 experiment decreased the survival rate of the Jewel Wasp*, Nasonia vitripennis*, eggs by 21% (Li et al., 2017). Even though my troubleshooting and experimentation efforts in this thesis were able to confirm transformed tissue in G0s, I was unable to produce a transgenic lineage (Table 5).

It is important that future attempts to use the CRISPR/Cas9 system in mosquitos consider the lessons learned from this prior research when trying to create transgenic lineages. Using optimal reagent concentrations and the most efficient sgRNAs, while incorporating clear phenotypic markers, seems to be key in streamlining experiments with small workforces. Additionally, simultaneous injections of multiple sgRNA targeting different areas within a loci of interest can avoid regions that seem resistant to cuts or

the use of inactive sgRNA. This can also expedite the screening process by allowing for diagnosis via varied PCR transcript lengths. When comparing the published use of the CRISPR/Cas9 system in *A. aegypti* to the <0.1% success rate using ZFNs, it is reasonable CRISPR/Cas9 should be considered the method-of-choice for convenient and effective genetic manipulation (Vosshall et al., 2013; Basu 2015).

Materials and Methods:

As a goal of this effort was to optimize the CRISPR/Cas9 system in *A. aegypt*i, my methodology changed slightly with experience. I was able to create G0 transgenic mosquitoes and provide a foundation from which future work can be built upon. Due to the apparent reduced success rate seen in studies that used plasmid Cas9/sgRNAs, I used protein Cas9 and preformed guide RNAs (Dong et al., 2015). A sgRNA for IR25a, and IR40a each were created by Maria Irigoyen to target the genomic sequences in Table 3. The microinjection rigs were kindly shared by the Bradley White, Peter Atkinson and the Omar Akbari Labs at UCR. Tom Guda of the Ray Lab taught mosquito husbandry, and Ming Lee of the White Lab mentored me in microinjections.

Mosquito Rearing

The Orlando strain of *A. aegypti* from the Ray Lab stock was used in these experiments. Mosquitoes were raised at 27° Celsius and 70% humidity with a 14:10 hour light-dark cycle at the UCR Insectary. Trays of a ~300–500 larvae were fed one Tetramin Fish Tropical Tablets (Catalog# 16110-03) pellet daily, water was replaced daily, and all

resultant pupa were allowed to eclose in 1 ft^3 insect cages. Adults were provided a 10% sucrose diet and allowed to breed for approximately three days before being blood-fed with Bovine Blood using a feeding apparatus from Hemostat Laboratories (Catalog# DBB500). The addition of a used human sock near the blood-feeding cages increased the feeding rate. Three to four days post-blood-feeding, the mosquitoes were isolated into vials of ~10 females and allowed to lay eggs on wet filter-paper. The largest, and presumably most fit, females were prioritized for use.

CRISPR/Cas9 injections

The microinjection methodology I used was mostly based upon the techniques established in the Vosshall Lab (Vosshall et al.; 2011; Kistler et al., 2014). Success rates changed as my experimentation progressed, likely due to my improvement in performing the techniques. Many factors outside of my control—such as the weather (the mosquitos would lay fewer eggs when it was raining), the mating success of individual mosquitoes (some seemed to lay more deformed eggs), the degree to which the mosquitoes would blood-feed and a host of other variables—influenced the success rate in unpredictable ways.

Silicate needles derived from Drummond Scientific Calibrated Micropipettes (Catalog# 21-180-18) were used to deliver the reagents during the first IR40a mutation attempt. Silicate needles, however, have the tendency to bend and the tips often broke non-uniformly. This was later remedied by using quartz needles (Catalog# QF100-70-10),

instead. To decrease the frequent needle clogging, quartz needles were coated by leaving the pre-pulled needles in a vacuum chamber near a 10 mL beaker containing one mL of Sigmacote (Catalog# SL2-100ML) for an hour. The sgRNA and Cas9, which were stored at -80° Celsius, were loaded into the needles and kept on ice with minimal light exposure during the experiment. FemtoJet injection rigs (Catalog# SM325) were initially used for injections, but were later replaced with PV820 Pneumatic Picopumps (Catalog# SYS-PV820). An injection pressure of 20–50 PSI, depending on the size of the needle tip, was used for injections, supplying approximately one-tenth of the egg's volume worth of injectant. Cas9 protein at a concentration of ~300 ng/µL was used for the first attempts to make IR40a and IR25a mutants, and ~200 ng/µL for subsequent injections. sgRNAs at a concentration of ~40 ng/µL were used. The reagents were diluted in fresh molecular-grade diH20 directly before the injection procedure and kept on ice.

After eggs were collected on wet filter-paper (Figure 12), they were kept in the dark for 15–45 minutes prior to injection. Once exposed to light, the melanization process began. As per established technique, eggs were allowed to melanize to a light-grey/purple color for the Fall and Winter 2015 IR40a and IR25a injection process. For subsequent runs, the eggs were injected at an earlier white/light-grey color (Figure 13A). Injecting the mosquito eggs at a slight angle (Figure 13B) improved survival as this decreased the deformation of eggs and reduced the size of the puncture wound left by the needle.

Eggs were lined up with their posterior ends against a filter-paper on top of a glass slide using fine paint brushes. I switched to Nitrocellulose Membrane (Catalog# 77010) in subsequent runs as it was more effective in regulating humidity, although it increased time required to line them up due to less amenable capillary forces. Dry filter-paper was then applied to the first piece of paper, and both papers were removed, causing the water to be removed, as well, while leaving the line of eggs. The eggs were allowed to dry for ~15 seconds before a coverslip with double-sided tape was used to pick up the eggs by laying the tape on the eggs with slight pressure. The eggs on the coverslip were then covered in Halocarbon Oil 27 (Catalog# H8773-100ML). Successful timing was confirmed by a less prominent chorion and a lack of desiccation. When too much time took place to get the eggs to the stage for microinjections, the chorion would thicken and cause the needles to break and clog (Figure 13). The use of double sided tape was later replaced by Tegaderm (Catalog# NC9634525) for greater sterility. Lined eggs under halocarbon oil were then immediately injected with the reagent mix; each needle was able to inject ~30 eggs.

After injections, the Halocarbon Oil 27 was removed by gently spraying diH20 above the eggs. Originally, the eggs were allowed to vertically dry in a moist chamber for a few hours as per the Vosshall procedure, but this was later replaced by floating the egg-covered coverslip on a wet filter paper within a parafilm-sealed petri dish with a small puncture hole in the parafilm. These petri dishes were allowed to incubate in a 25° Celsius, 60% humidity incubator for approximately two days before the coverslip was

removed and submerged in water trays. Greater hatch rates were achieved by the addition of a small amount of water taken from trays of newly hatched *A. aegypti* eggs. After all eggs hatched naturally, any eggs that did not hatch were placed in a vacuum chamber for approximately one hour, which reliably caused more eggs to hatch. Emerged larvae were then raised under normal conditions.

In order to achieve successful lineage of mutant strains from their G0 predecessors, individual pupa were eclosed in containers that included egg-laying cups and 10% sucrose food cups. Emerging virgins were then mated to approximately three wild-type mosquitoes of the opposite sex, blood-fed and allowed to lay eggs, which were then collected as G1s (Figure 11B). Second blood-feedings and egg collections were performed to increase the chance of collecting viable eggs. ~50–65 G1 progeny were raised, mated, blood-fed and had their eggs collected and hatched while the G1 adults were used for genotyping.

Genotyping

In the first attempt to create IR40a and IR25a mutants via the CRISPR/Cas9 system, G0s were collected and used for genotyping to confirm the successful transformation of tissue (Figures 15 and 16). Following confirmation that successful transformation had occurred using these reagents and restriction digest analysis, genotyping was then only performed on the G1s after the G2 eggs were collected. Genotyping consisted of isolating genomic DNA from individual mosquitoes, using 75 µL

of gDNA extraction solution (10 mM Tris-HCl, 5mM EDTA, 25mM NaCl and 200 µg/mL Protein Kinase B). Genomic material was then used in an amplification employing Dreamtaq Green PCR Master Mix (Catalog# K1081) and Accupower PCR Master Mix (Catalog# K-2011) restriction digest using the primers (Table 4), and New England Biolabs restriction enzymes Mnl1 (Catalog# R0163S) and Sty1 (Catalog# R0500S) as seen in Figure 15. Mosquito tissue was considered to be successfully transformed if the fragment could not be digested with the appropriate restriction enzyme.

Results:

The results demonstrate that transgenic tissue in *A. aegypti* G0s could be created for the genes IR40a and IR25a using the CRISPR/Cas9 system. I was reliably able to produce G0 survivors with transgenic tissue. Similar to previous findings, Table 5 shows the different genes that were targeted with unique sgRNA may have induced different heartiness in the mosquitoes. IR40a and IR25a targeted G0 had survival rates, 10–13%, comparable to publications using the CRISPR/Cas9 system in *A. aegypti* who had not optimized their choice of sgRNA (Dong et al., 2015; Gantz et al., 2015; Kistler et al., 2014). Likewise, G0 transgenic rates, ~25% in the first runs, were comparable, if not on the upper range, to the previously referenced literature. These rates, however, were lower than literature where the sgRNA had been optimized. Like other labs, G0s were noticed to be far less fertile than wild-type (Basu et al., 2015).

Discussion:

By inference of results, slight changes in protocol can increase survivability of G0s altered by a CRISPR/Cas9 system. We anticipate that injecting younger embryos produces fewer survivors, but would have the greatest rates of transformation. This is conceptually consistent with the results of labs who found earlier injection times improved the results of CRISPR/Cas9 efficacy in butterflies (Li et al., 2015; Zhang & Reed, 2017). From observations, quartz needles layered in Sigmacote both improved the speed of the injection process and decreased the damage to the embryos by reducing needle clogging. Genotyping via restriction digest seems to be an effective way to distinguish CRISPR/Cas9-induced INDELs in individual mosquitoes. When vacuum chambers were used and/or water from used hatching trays was added to immersed eggs, the rate of larval emergence was immediately observed to increase, consistent with previous literature (Horsfall, Lum, & Henderson, 1958). The survival rates only slightly increased between my first and second attempts at creating IR25a and IR40a mutants. This is reasonable, as my technique and materials improved, I was also injecting at an earlier time after the eggs were laid (Figure 13). Because a variety of factors were changed over a small number of runs, it is difficult to objectively pinpoint exactly which aspects changed. However, the ~24% G0 mutation rate of my first CRISPR/Cas9 attempts, calculated by the ratio of individuals with transformed tissue to eclosed mosquitoes, indicates a very promising start in the effort to create IR mutant *A. aegypti*.

Based upon these experiences, I believe that the CRISPR/Cas9 system is a viable tool for creating transgenic *A. aegypti* with mutant IR genes. It is advisable to test many sgRNA in order to find highly efficient guide sequences (Kistler et al., 2014). It is also advised to use ~200–300 ng/µL of Cas9 (in the protein form) and ~40 ng/µL of sgRNA transcripts when injecting *A. aegypti* (Kistler et al., 2014). Raising up to a thousand G1s will likely ensure a good chance for identifying instances of germline transmission, especially when the goal is to induce HDR insertions or excisions (Gantz et al., 2015). Without obvious markers of mutation, or if mutations cause the specimen to be unhealthy, greater numbers will be required to establish and test transgenic lines. There is a vast degree of variability between success rates of studies testing the CRISPR/Cas9 system in different species of mosquitoes, as well.

The CRISPR/Cas system has proved to be valuable as it allows rapid, precise and cheap genetic manipulation. However, I experienced an initial period of fine-tuning. It was recognized at the start the project that using the CRISPR/Cas9 to create INDEL IR40a and IR25a mutant *A. aegypti* was a gamble. Exploration using non-model organisms means foregoing the massive advantage of having specific Cas9 expressing strains, like those established in *D. melanogaster*. Despite the promise of this new technology, prior studies still required significant investment in time and resources to obtain any meaningful results. Additionally, much of the prior research benefited from the goal of just aiming to provide “proof of concept.” They set out to create knockouts, insert clear reporter genes, raise extremely large pools of G0s and G1s, and use High Resolution

Melt analysis detect mutation events rather than trying to establish mutant lineages. This minimizes the impediments associated with the labor-intensive process of raising and breeding individual mosquitoes. This makes it unsurprising that, in my small-scale runs using low numbers of specimen, I was not able to establish a transgenic lineage. This process still yielded valuable information on transformation efficiency of the sgRNA used. For future research, we must consider that the guide RNAs for IR25a included an SNP. It is not known to what degree this may have influenced my results. We were able to see, as were the other scientists attempting to perform CRISPR/Cas9 on *A. aegypti*, that some sgRNA were vastly less successful than others, but that the system is still a viable means to produce transgenic tissue in this disease vector species.

Conclusion

My work contributes to the recent and growing investigation of IRs in insects, as well as the efforts to manipulate genes using the state-of-the-art CRISPR/Cas9 system. This research has helped to lay the groundwork for future characterization of the roles of these genes and the creation of useful transgenic lines for both research and practical application. My time in the Ray Lab at UCR, including work not presented, has provided me with a broad skillset to pursue a career in research.

References

AAEL009813 - AAEL009813-PA - Aedes aegypti (Yellowfever mosquito) - AAEL009813 gene & protein. (2017). *Uniprot.org*. Retrieved 13 February 2017, from http://www.uniprot.org/uniprot/Q16US4.

AAEL006360 - AAEL006360-PA - Aedes aegypti (Yellowfever mosquito) - AAEL006360 gene & protein. (2017). *Uniprot.org*. Retrieved 13 February 2017, from http://www.uniprot.org/uniprot/Q176J1.

AAEL014270 - AAEL014270-PA - Aedes aegypti (Yellowfever mosquito) - AAEL014270 gene & protein. (2017). *Uniprot.org*. Retrieved 13 February 2017, from http://www.uniprot.org/uniprot/Q16GT6.

Abuin, L., Bargeton, B., Ulbrich, M., Isacoff, E., Kellenberger, S., & Benton, R. (2011). Functional Architecture of Olfactory Ionotropic Glutamate Receptors. *Neuron*, *69*(1), 44-60, http://dx.doi.org/10.1016/j.neuron.2010.11.042.

Addgene: CRISPR/Cas9 Guide. (2017). *Addgene.org*. Retrieved 28 February 2017, from https://www.addgene.org/crispr/guide/#plan-experiment.

Altner, H., Tichy, H., & Altner, I. (1978). Lamellated Outer Dendritic Segments of a Sensory Cell within a Poreless Thermo- and Hygroreceptive Sensillum of the Insect Carausius morosus. *Cell and Tissue Research*, *191*(2), http://dx.doi.org/10.1007/bf00222425.

Barbagallo, B., & Garrity, P. (2015). Temperature Sensation in Drosophila. *Current Opinion in Neurobiology*, *34*(1), 8-13, http://dx.doi.org/10.1016/j.conb.2015.01.002.

Barrangou, R., Fremaux, C., Deveau, H., Richards, M., Boyaval, P., & Moineau, S., … Horvath, P. (2007). CRISPR Provides Acquired Resistance Against Viruses in Prokaryotes. *Science*, *315*(5819), 1709-1712, http://dx.doi.org/10.1126/science.1138140.

Basu, S., Aryan, A., Overcash, J., Samuel, G., Anderson, M., & Dahlem, T., … Adelman, Z. (2015). Silencing of End-joining Repair for Efficient Site-specific Gene Insertion After TALEN/CRISPR Mutagenesis in Aedes aegypti. *Proceedings of The National Academy of Sciences*, *112*(13), 4038-4043, http://dx.doi.org/10.1073/pnas.1502370112.

Benton, R., Vannice, K., Gomez-Diaz, C., & Vosshall, L. (2009). Variant Ionotropic Glutamate Receptors as Chemosensory Receptors in Drosophila. *Cell*, *136*(1), 149-162, http://dx.doi.org/10.1016/j.cell.2008.12.001.

Boxshall, G. (2004). The Evolution of Arthropod Limbs. *Biological Reviews*, *79*(2), 253-300. http://dx.doi.org/10.1017/s1464793103006274.

Callaway, E. (2017). *HIV overcomes CRISPR Gene-editing Attack*. *Nature News*. Retrieved 28 February 2017, from http://www.nature.com/news/hiv-overcomes-crispr-gene-editing-attack-1.19712.

Cameron, P., Hiroi, M., Ngai, J., & Scott, K. (2010). The Molecular Basis for Water Taste in Drosophila. *Nature*, *465*(7294), 91-95, http://dx.doi.org/10.1038/nature09011.

Carvalho, D., McKemey, A., Garziera, L., Lacroix, R., Donnelly, C., & Alphey, L., … Capurro, M. (2015). Suppression of a Field Population of Aedes aegypti in Brazil by Sustained Release of Transgenic Male Mosquitoes. *PLOS Neglected Tropical Diseases*, *9*(7), e0003864. http://dx.doi.org/10.1371/journal.pntd.0003864.

Croset, V., Rytz, R., Cummins, S., Budd, A., Brawand, D., & Kaessmann, H., … Benton, R. (2010). Ancient Protostome Origin of Chemosensory Ionotropic Glutamate Receptors and the Evolution of Insect Taste and Olfaction. *Plos Genetics*, *6*(8), e1001064, http://dx.doi.org/10.1371/journal.pgen.1001064.

Cassidy, A., van Steensel, M., Steijlen, P., van Geel, M., van der Velden, J., & Morley, S., … Terrinoni, A. (2005). A Homozygous Missense Mutation in TGM5 Abolishes Epidermal Transglutaminase 5 Activity and Causes Acral Peeling Skin Syndrome. *The American Journal of Human Genetics*, *77*(6), 909-917, http://dx.doi.org/10.1086/497707.

Cumming, G., Fidler, F., & Vaux, D. (2007). Error Bars in Experimental Biology. *The Journal of Cell Biology*, *177*(1), 7-11, http://dx.doi.org/10.1083/jcb.200611141.

Dong, S., Lin, J., Held, N., Clem, R., Passarelli, A., & Franz, A. (2015). Heritable CRISPR/Cas9-Mediated Genome Editing in the Yellow Fever Mosquito, Aedes aegypti. *PLOS ONE*, *10*(3), e0122353. http://dx.doi.org/10.1371/journal.pone.0122353.

Enjin, A., Zaharieva, E., Frank, D., Mansourian, S., Suh, G., Gallio, M., & Stensmyr, M. (2016). Humidity Sensing in Drosophila. *Current Biology*, *26*(10), 1352-1358. http://dx.doi.org/10.1016/j.cub.2016.03.049.

Foelix, R., Stocker, R., & Steinbrecht, R. (1989). Fine Structure of a Sensory Organ in the Arista of Drosophila melanogaster and Some Other Dipterans. *Cell and Tissue Research*, *258*(2), http://dx.doi.org/10.1007/bf00239448.

Freeman, E., & Dahanukar, A. (2015). Molecular neurobiology of Drosophila taste. *Current Opinion in Neurobiology*, *34*, 140-148, http://dx.doi.org/10.1016/j.conb.2015.06.001.

Fuss, S., & Ray, A. (2009). Mechanisms of Odorant Receptor Gene Choice in Drosophila and Vertebrates. *Molecular and Cellular Neuroscience*, *41*(2), 101-112, http://dx.doi.org/10.1016/j.mcn.2009.02.014.

Gan, H., Tan, M., Gan, H., Lee, Y., & Austin, C. (2015). The Complete Mitogenome of the Norway lobster Nephrops norvegicus (Linnaeus, 1758) (Crustacea: Decapoda: Nephropidae). *Mitochondrial DNA*, *27*(5), 1-2, http://dx.doi.org/10.3109/19401736.2015.1007325.

Gantz, V., Jasinskiene, N., Tatarenkova, O., Fazekas, A., Macias, V., Bier, E., & James, A. (2015). Highly Efficient Cas9-mediated Gene Drive for Population Modification of the Malaria Vector Mosquito Anopheles stephensi. *Proceedings of The National Academy of Sciences*, *112*(49), E6736-E6743. http://dx.doi.org/10.1073/pnas.1521077112.

Gasiunas, G., Barrangou, R., Horvath, P., & Siksnys, V. (2012). Cas9-crRNA Ribonucleoprotein Complex Mediates Specific DNA Cleavage for Adaptive Immunity in Bacteria. *Proceedings of The National Academy of Sciences*, *109*(39), E2579-E2586. http://dx.doi.org/10.1073/pnas.1208507109.

Hammond, A., Galizi, R., Kyrou, K., Simoni, A., Siniscalchi, C., & Katsanos, D., Nolan, T. (2015). A CRISPR-Cas9 Gene Drive System Targeting Female Reproduction in the Malaria Mosquito Vector Anopheles gambiae. *Nature Biotechnology*, *34*(1), 78-83, http://dx.doi.org/10.1038/nbt.3439.

Harris, A., Nimmo, D., McKemey, A., Kelly, N., Scaife, S., & Donnelly, C. et al. (2011). Field Performance of Engineered Male Mosquitoes. *Nature Biotechnology*, *29*(11), 1034-1037. http://dx.doi.org/10.1038/nbt.2019.

Horsfall, W., Lum, P., & Henderson, L. (1958). Eggs of Floodwater Mosquitoes (Diptera: Culicidae) V. Effect of Oxygen on Hatching of Intact Eggs. *Annals of The Entomological Society of America*, *51*(2), 209-213. http://dx.doi.org/10.1093/aesa/51.2.209.

Inoshita, T., & Tanimura, T. (2006). Cellular Identification of Water Gustatory Receptor Neurons and their Central Projection Pattern in Drosophila. *Proceedings of The National Academy of Sciences*, *103*(4), 1094-1099. http://dx.doi.org/10.1073/pnas.0502376103.

Ji, F., & Zhu, Y. (2015). A Novel Assay Reveals Hygrotactic Behavior in Drosophila. *PLOS ONE*, *10*(3), e0119162. http://dx.doi.org/10.1371/journal.pone.0119162.

Kistler, K., Vosshall, L., & Matthews, B. (2014). Genome-engineering with CRISPR-Cas9 in the Mosquito Aedes aegypti. *Biorxiv Beta*. http://dx.doi.org/10.1101/013276.

Knecht, Z., Silbering, A., Ni, L., Klein, M., Budelli, G., & Bell, R., … Samuel, D. (2016). Distinct Combinations of Variant Ionotropic Glutamate Receptors Mediate Thermosensation and Hygrosensation in Drosophila. *Elife*, *5*, http://dx.doi.org/10.7554/elife.1787.

Krafsur, E., Whitten, C., & Novy, J. (1987). Screwworm Eradication in North and Central America. *Parasitology Today*, *3*(5), 131-137. http://dx.doi.org/10.1016/0169-4758(87)90196-7.

Lander, E. (2016). The Heroes of CRISPR. *Cell*, *164*(1-2), 18-28. http://dx.doi.org/10.1016/j.cell.2015.12.041.

Li, M., Au, L., Douglah, D., Chong, A., White, B., Ferree, P., & Akbari, O. (2017). Generation of Heritable Germline Mutations in the Jewel Wasp Nasonia vitripennis using CRISPR/Cas9. *Scientific Reports*, *7*(1), http://dx.doi.org/10.1038/s41598-017-00990-3.

Li, X., Fan, D., Zhang, W., Liu, G., Zhang, L., & Zhao, L., … Wang, W. (2015). Outbred Genome Sequencing and CRISPR/Cas9 Gene Editing in Butterflies. *Nature Communications*, *6*, 8212, http://dx.doi.org/10.1038/ncomms9212.

Liu, L., Li, Y., Wang, R., Yin, C., Dong, Q., & Hing, H., … Welsh, M. (2007). Drosophila Hygrosensation Requires the TRP channels Water Witch and Nanchung. *Nature*, *450*(7167), 294-298. http://dx.doi.org/10.1038/nature06223.

Luz, C., & Fargues, J. (1999). Dependence of the Entomopathogenic Fungus, Beauveria bassiana, on High Humidity for Infection of Rhodnius prolixus. *Mycopathologia*, *146*(1), 33-41. http://dx.doi.org/10.1023/a:1007019402490.

Missbach, C., Dweck, H., Vogel, H., Vilcinskas, A., Stensmyr, M., Hansson, B., & Grosse-Wilde, E. (2014). Evolution of Insect Olfactory Receptors. *Elife*, *3*, http://dx.doi.org/10.7554/elife.02115.

Montague, T., Cruz, J., Gagnon, J., Church, G., & Valen, E. (2014). CHOPCHOP: a CRISPR/Cas9 and TALEN Web Tool for Genome Editing. *Nucleic Acids Research*, *42*(W1), W401-W407. http://dx.doi.org/10.1093/nar/gku410.

Montell, C. (2008). TRP Channels: It's Not the Heat, It's the Humidity. *Current Biology*, *18*(3), R123-R126. http://dx.doi.org/10.1016/j.cub.2007.12.001.

Ni, L., Klein, M., Svec, K., Budelli, G., Chang, E., & Ferrer, A. et al. (2016). The Ionotropic Receptors IR21a and IR25a Mediate Cool Sensing in Drosophila. *Elife*, *5*, http://dx.doi.org/10.7554/elife.13254.

Pawluk, A., Bondy-Denomy, J., Cheung, V., Maxwell, K., & Davidson, A. (2014). A New Group of Phage Anti-CRISPR Genes Inhibits the Type I-E CRISPR-Cas System of

Pseudomonas aeruginosa. *Mbio*, *5*(2), e00896-14-e00896-14. http://dx.doi.org/10.1128/mbio.00896-14.

Potter, C. (2014). Stop the Biting: Targeting a Mosquito's Sense of Smell. *Cell*, *156*(5), 878-881. http://dx.doi.org/10.1016/j.cell.2014.02.003.

Protein BLAST: search protein databases using a protein query. (2017). *Blast.ncbi.nlm.nih.gov*. Retrieved 3 March 2017, from https://blast.ncbi.nlm.nih.gov/Blast.cgi?PROGRAM=blastp&PAGE_TYPE=BlastSearch&LINK_LOC=blasthome

Reardon, S. (2015). Leukemia Success Heralds Wave of Gene-editing Therapies. *Nature*, *527*(7577), 146-147. http://dx.doi.org/10.1038/nature.2015.18737.

Reuters, A. (2017). Brazil's Rousseff declares 'war' on the Aedes aegypti mosquito. *Buenosairesherald.com*. Retrieved 2 May 2017, from http://www.buenosairesherald.com/article/207692/brazil%E2%80%99s-rousseff-declares-%E2%80%98war%E2%80%99-on-the-aedes-aegypti--mosquito.

Robertson, H., Warr, C., & Carlson, J. (2003). Molecular Evolution of the Insect Chemoreceptor Gene Superfamily in Drosophila melanogaster. *Proceedings of The National Academy of Sciences*, *100*(Supplement 2), 14537-14542. http://dx.doi.org/10.1073/pnas.2335847100.

Rytz, R., Croset, V., & Benton, R. (2013). Ionotropic Receptors (IRs): Chemosensory Ionotropic Glutamate Receptors in Drosophila and Beyond. *Insect Biochemistry and Molecular Biology*, *43*(9), 888-897. http://dx.doi.org/10.1016/j.ibmb.2013.02.007.

Sayeed, O., & Benzer, S. (1996). Behavioral Genetics of Thermosensation and Hygrosensation in Drosophila. *Proceedings of The National Academy of Sciences*, *93*(12), 6079-6084. http://dx.doi.org/10.1073/pnas.93.12.6079.

Sengupta, P., & Garrity, P. (2013). Sensing Temperature. *Current Biology*, *23*(8), R304-R307. http://dx.doi.org/10.1016/j.cub.2013.03.009.

Shanbhag, S., Singh, K., & Singh, R. (1994). Fine Structure and Primary Sensory Projections of Sensilla Located in the Sacculus of the Antenna of Drosophila melanogaster. *Cell & Tissue Research*, *282*(2), 237-249. http://dx.doi.org/10.1007/bf00319115.

Sowell, R., Hersberger, K., Kaufman, T., & Clemmer, D. (2007). Examining the Proteome of Drosophila Across Organism Lifespan. *Journal of Proteome Research*, *6*(9), 3637-3647. http://dx.doi.org/10.1021/pr070224h.

Suzuki, K., Tsunekawa, Y., Hernandez-Benitez, R., Wu, J., Zhu, J., & Kim, E., … Lajara, J. (2016). In Vivo Genome Editing via CRISPR/Cas9 Mediated Homology-independent Targeted Integration. *Nature*, *540*(7631), 144-149. http://dx.doi.org/10.1038/nature20565.

TMHMM Server, v. 2.0. (2017). *Cbs.dtu.dk*. Retrieved 9 November 2016, from http://www.cbs.dtu.dk/services/TMHMM/.

Wexler, A., & Hasegawa, S. (1954). Relative Humidity-temperature Relationships of some Saturated Salt Solutions in the Temperature Range 0 Degree to 50 Degrees C. *Journal of Research of The National Bureau of Standards*, *53*(1), 19. http://dx.doi.org/10.6028/jres.053.003.

Wong, N., Liu, W., & Wang, X. (2015). WU-CRISPR: Characteristics of Functional Guide RNAs for the CRISPR/Cas9 System. *Genome Biology*, *16*(1). http://dx.doi.org/10.1186/s13059-015-0784-0.

Wu, Y., Liang, D., Wang, Y., Bai, M., Tang, W., & Bao, S., … Li, J. (2013). Correction of a Genetic Disease in Mouse via Use of CRISPR-Cas9. *Cell Stem Cell*, *13*(6), 659-662. http://dx.doi.org/10.1016/j.stem.2013.10.016.

Yao, C. (2005). Chemosensory Coding by Neurons in the Coeloconic Sensilla of the Drosophila Antenna. *Journal of Neuroscience*, *25*(37), 8359-8367. http://dx.doi.org/10.1523/jneurosci.2432-05.2005.

Zhang, L., & Reed, R. (2017). A Practical Guide to CRISPR/Cas9 Genome Editing in Lepidoptera. *Biorixiv*. http://dx.doi.org/10.1101/130344.

Zhou, X., Slone, J., Rokas, A., Berger, S., Liebig, J., & Ray, A. et al. (2012). Phylogenetic and Transcriptomic Analysis of Chemosensory Receptors in a Pair of Divergent Ant Species Reveals Sex-Specific Signatures of Odor Coding. *Plos Genetics*, *8*(8), e1002930. http://dx.doi.org/10.1371/journal.pgen.1002930.

Figure 1

Phylogenetic Analysis and Alignment of IR25a (BlastP-NIH, 2017)

IR25a demonstrated a high level of conservation among *A. gambiae, C. elegans, D. melanogaster and D. suzukii*. Similar sequences were found in humans and house mice. No appreciable homologues were found in *N. norvegicus*. Standard BLASTP cutoffs of E-threshold of 10 were used and images from NIH alignment programs are listed below. Species beyond this cutoff were not represented. (A) Similarity scores to Vectorbase-predicted amino acid sequence of *A. aegypti* IR25a with the greatest matching identities of each species represented. (B) Phylogenetic tree (unscaled) of predicted IR25a amino acid sequences (*A. aegypti* in yellow). (C) Amino acid alignment of sequences most similar to *A. aegypti* IR25a for each species within the E-threshold cutoff. Matching sequences are in red.

(A)

Description	Max score	Total score	Query cover	E value	Ident
AAEL009813-PA *Aedes aegypti*	1895	1895	100%	0.0	100%
AGAP010272-PA *Anopheles gambiae*	1569	1569	99%	0.0	82%
PREDICTED: glutamate receptor 4 *Drosophila suzukii*	1390	1390	99%	0.0	72%
IP13516p *Drosophila melanogaster*	1384	1384	99%	0.0	72%
GLutamate Receptor family (AMPA) *Caenorhabditis elegans*	648	648	89%	0.0	45%
glutamate receptor ionotropic, kainate 1 isoform 5 *Homo sapiens*	295	295	55%	5e-86	33%
kainate receptor GluR7 3 subunit *Mus musculus*	287	287	50%	1e-85	36%

(B)

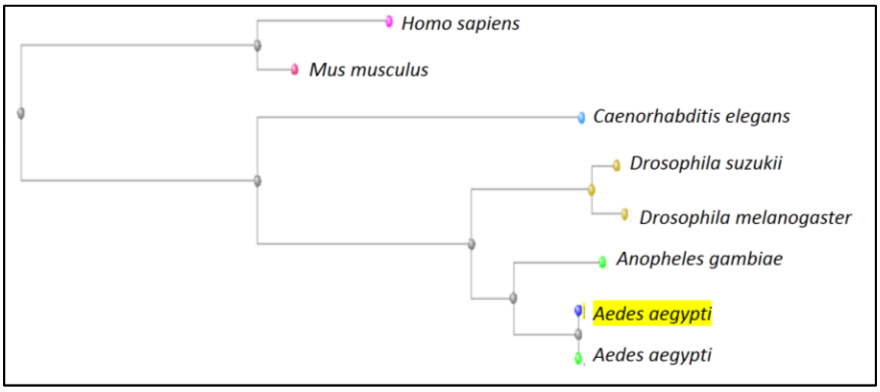

(C)

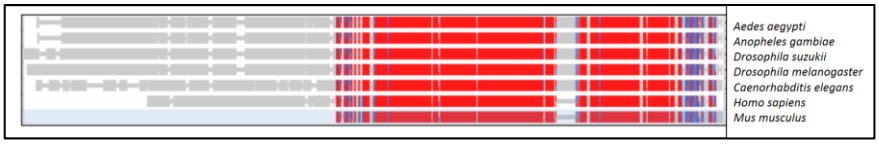

Figure 2

Phylogenetic Analysis and Alignment of IR40a (BlastP-NIH, 2017).

IR40a demonstrated a high level of conservation among *A. gambiae, C. elegans, D. melanogaster and D. suzukii*. No appreciable homologues were found in humans, house mice and *N. norvegicus*. Standard BLASTP cutoffs of E-threshold of 10 were used and images from NIH alignment programs are listed below. Species beyond this cutoff were not represented. (A) Similarity scores to Vectorbase-predicted amino acid sequence of *A. aegypti* IR40a with the greatest matching identities of each species represented. (B) Phylogenetic tree (unscaled) of predicted IR40a amino acid sequences (*A. aegypti* in yellow). (C) Amino acid alignment of sequences most similar to *A. aegypti* IR40a for each species within the E-threshold cutoff. Matching sequences are in red.

(A)

Description	Max score	Total score	Query cover	E value	Ident
AAEL014270-PA *Aedes aegypti*	1596	1596	100%	0.0	100%
AGAP004021-PA *Anopheles gambiae*	858	858	83%	0.0	62%
Ionotropic receptor 40a, isoform F *Drosophila melanogaster*	490	490	82%	4e-162	39%
PREDICTED: uncharacterized protein LOC108005942 *Drosophila suzukii*	347	347	55%	5e-110	43%

(B)

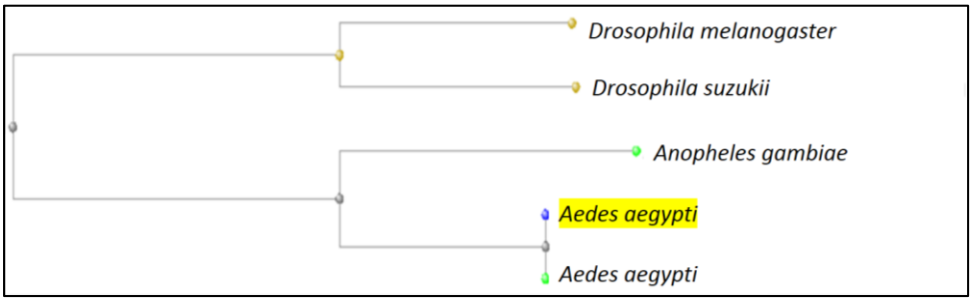

(C)

Figure 3

Sequence Confirmation of *IR40a(6)* and *IR40a(7)* Mutants

Fragments of 682-719 base pairs in *D. melanogaster* IR40a. Retrogen sequences of *IR40a(6)* and *IR40a(7)* mutants from Ray Lab stock.

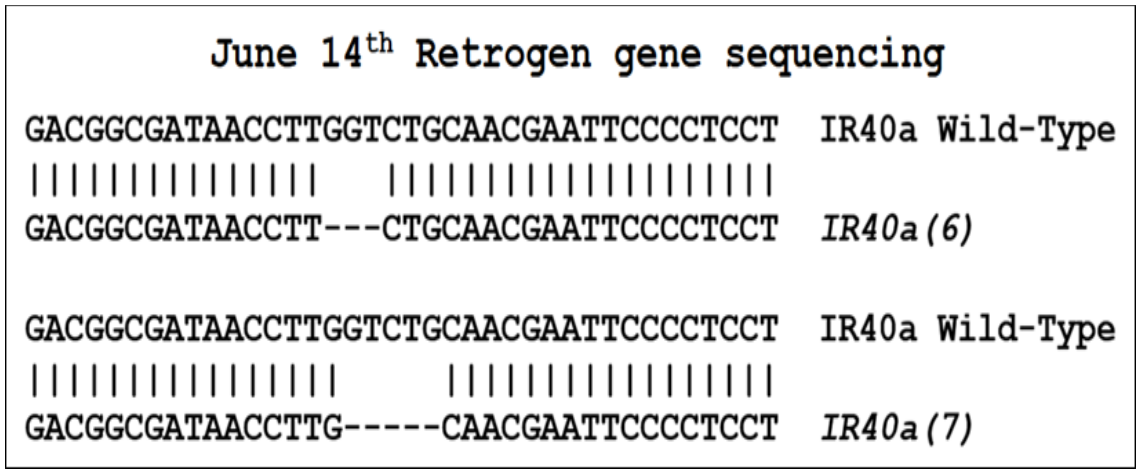

Figure 4

Alignment of IR40a in Insect Species

Amino acid sequence alignment of multiple insect species demonstrated conservation of the IR40a gene. The INDEL target of the Ray Lab CRISPR IR40a mutants is highlighted in blue.

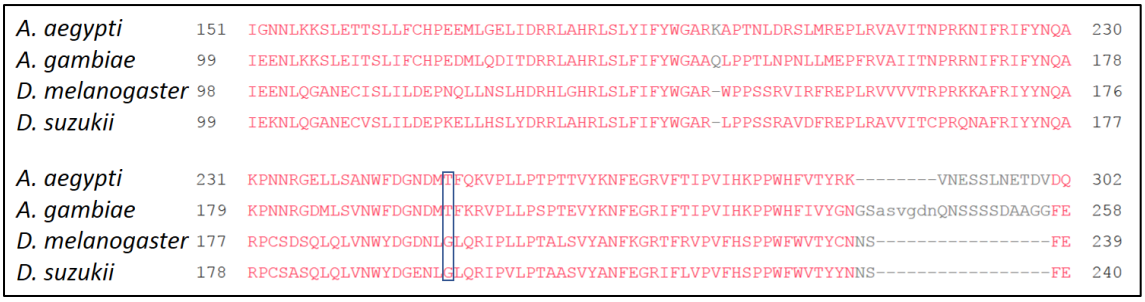

Figure 5

Analysis of *IR40a(6)* Mutant *D. melanogaster*

Alignment of *D. melanogaster IR40a(6)* mutant and predicted changes in functional domains. Ray Lab CRISPR generated *IR40a(6)* mutants contain a missing Glycine amino acid at the 196th position. TMHMM 2.0 predicted no changes in the transmembrane structure of the *IR40a(6)* mutant.

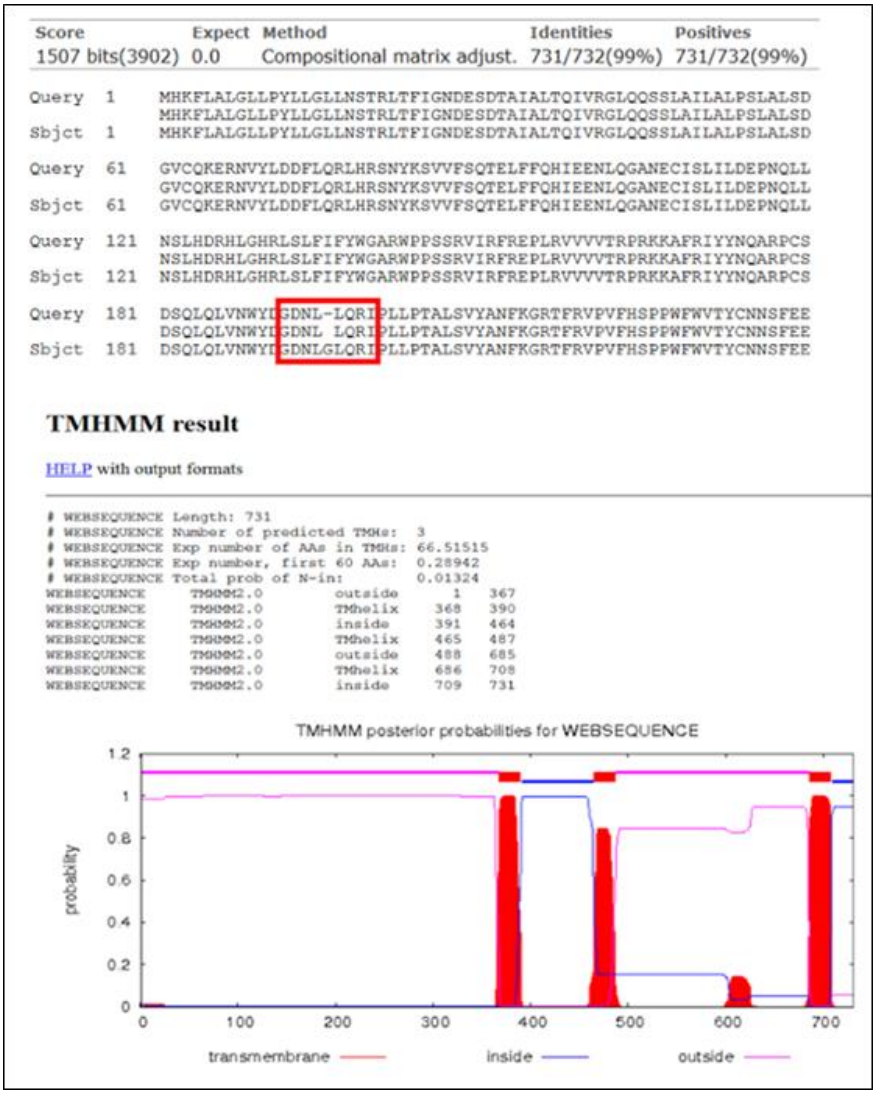

Figure 6

Analysis of *IR40a(7)* Mutant *D. melanogaster*

Alignment of *D. melanogaster IR40a(7)* mutant and predicted changes in functional domains. Ray Lab CRISPR generated *IR40a(7)* mutants contain a five-nucleotide deletion at the 697th nucleotide position. TMHMM 2.0 predicted a vast loss in the transmembrane structure of the *IR40a(7)* mutant.

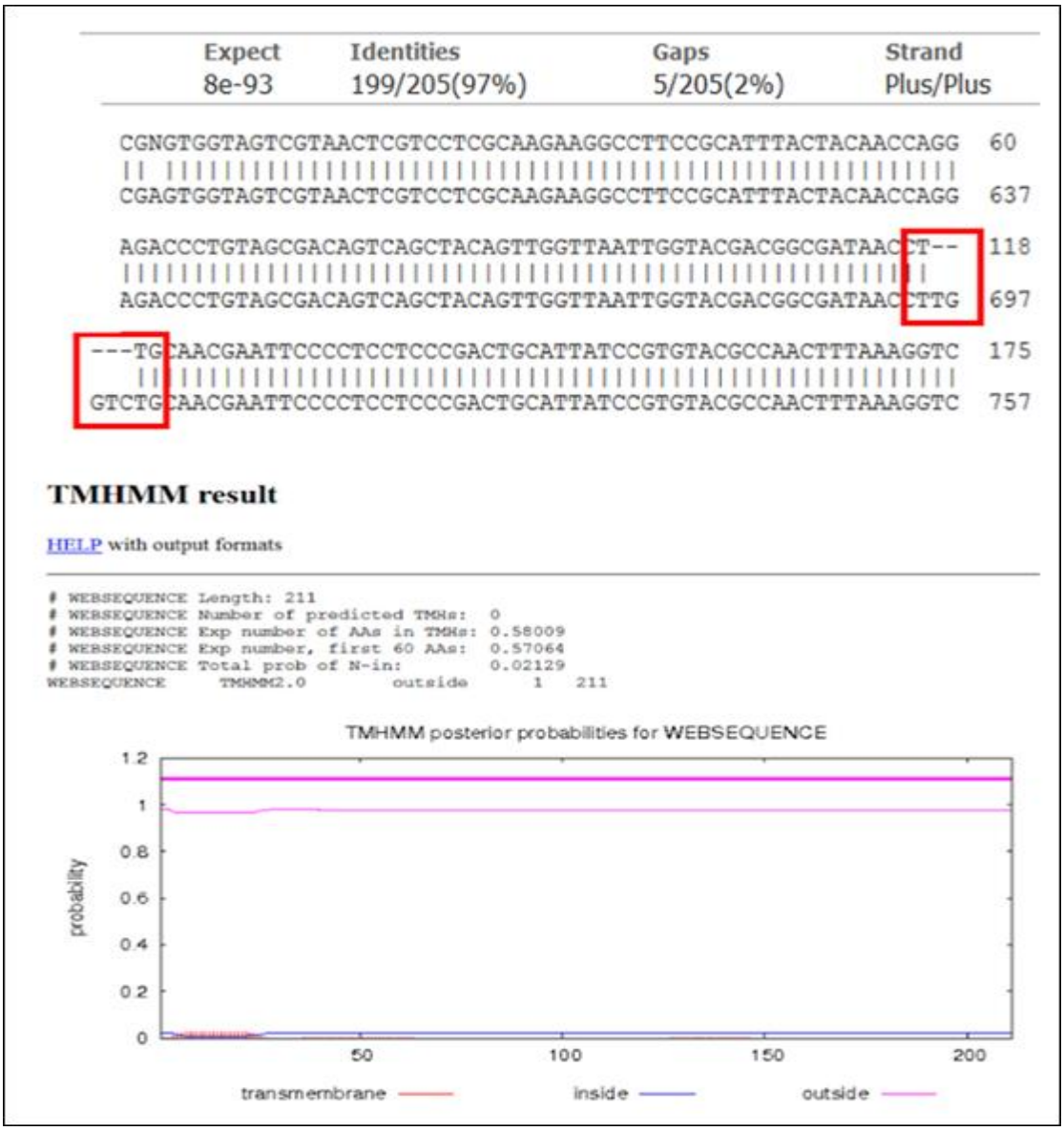

Figure 7

Representation of Knecht et al. and Enjin's et al.s' (2016) Humidity Gradient Behavioral Assays Results

Arrows represent the direction of mutant IR flies' behavior in humidity gradient behavioral assays. The scale represents 0–100% RH. Extremes of the arrows represent the two humidity options of the two-choice assay. Width of arrows represents the degree of behavioral influence when the adjacent gene was inhibited. Wider arrows represent stronger behavioral influence. The green arrow represents the Knecht et al. (2016) results. Red arrows represent the Enjin et al. (2016) results. The star denotes the approximate optimal humidity for *D. melanogaster*.

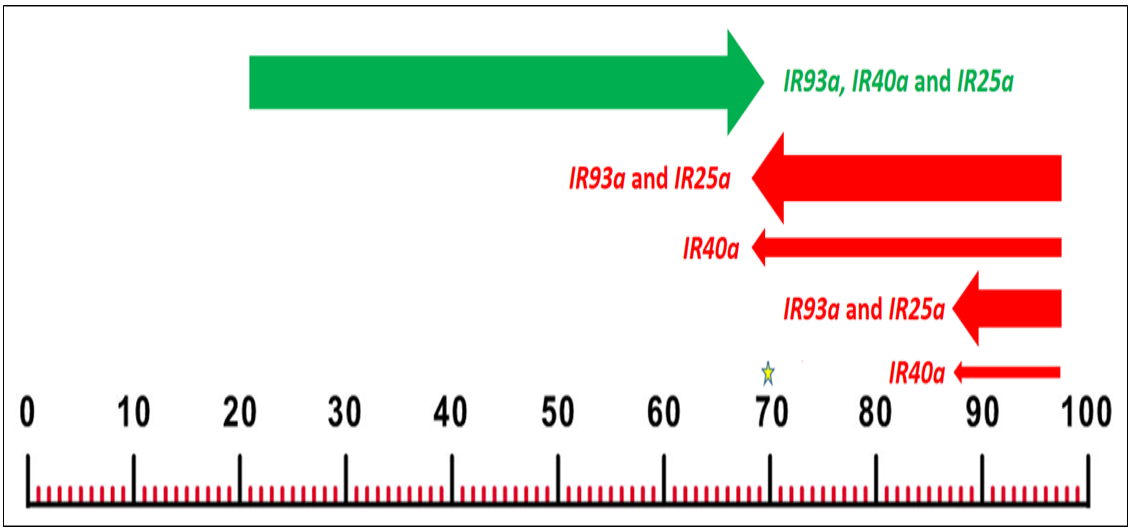

Figure 8

Humidity Gradient Behavioral Assay Rigs of Knecht et al. and Enjin et al. (2016)

Replicated humidity gradient behavioral assay rigs according to Knecht et al. (2016) (right) and Enjin et al. (2016) (left) papers' methodologies. Enjin et al. (2016), used a 3D printed lid, dividing the plate into lanes, as well as a lighting source from below the plates, both of which were not replicated. Differences included plate lid material, Parafilm, tape and a hole in the lid.

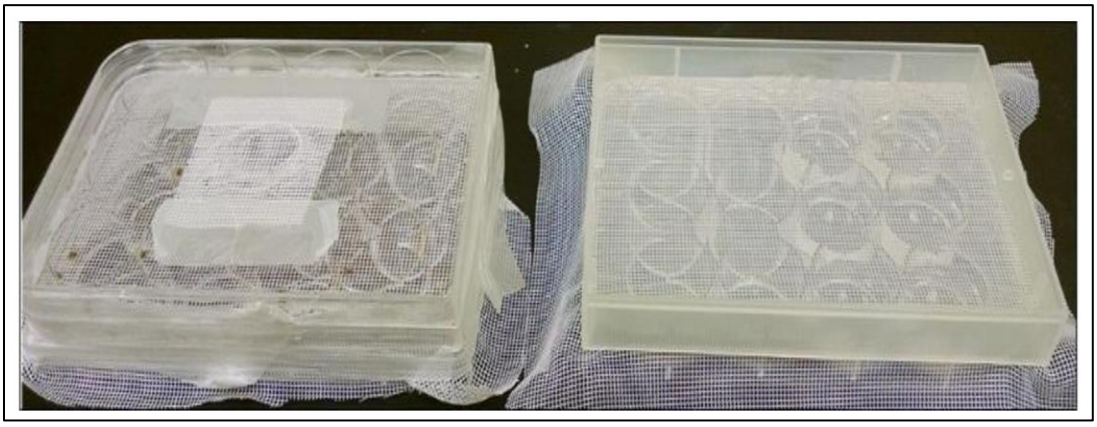

Figure 9

Humidity Gradient Behavioral Assays

Screenshots of plates used during my assays. (A) Closeup of two strains being tested. (B) Screenshot of the testing area (white-paper-lined open-top box surrounding the assay not shown).

(A)

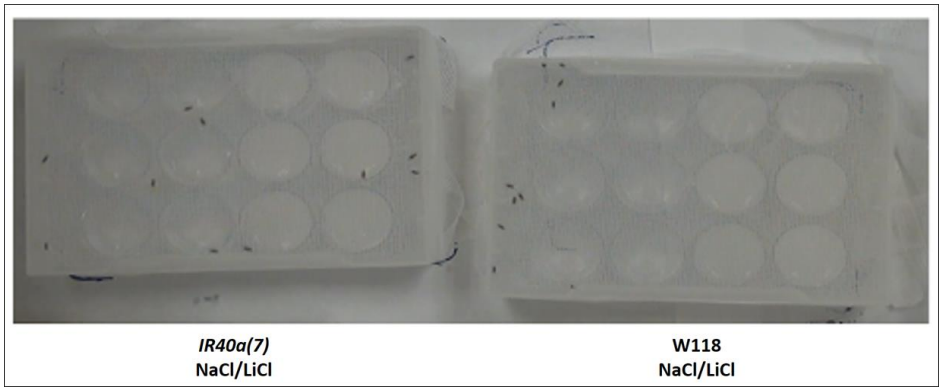

(B)

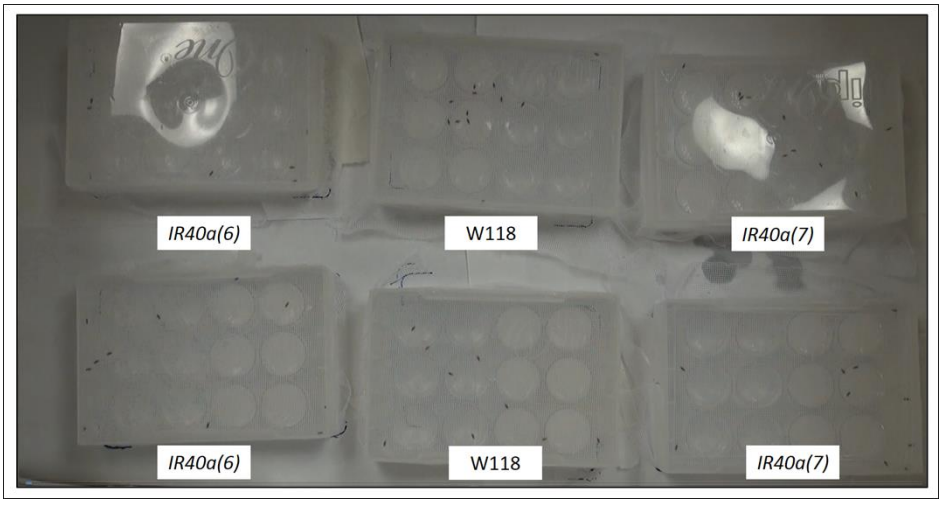

Figure 10

Graphical Illustration of PI Results

Mean Preference Indexes of my humidity gradient behavioral assays testing NaCl/NaCl (70/70% RH) and LiCl/NaCl (20/70% RH) gradients with *D. melanogaster* wild-type and mutants over a four-hour time period (SEM bars). (A) W118 Canton-S control. (B) *OR83b(2)* control. (C) *IR40a(6)* (single amino acid deletion). (D) *IR40a(7)* (five-nucleotide deletion).

(A)

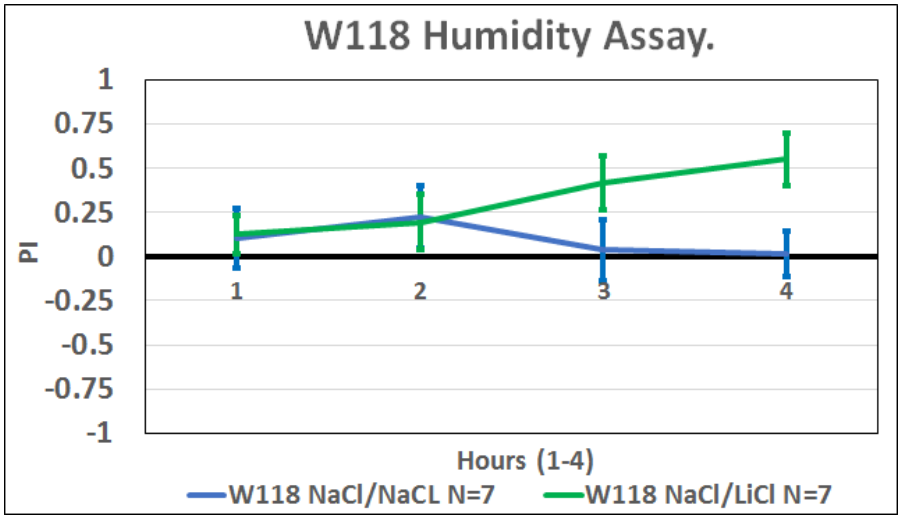

(B)

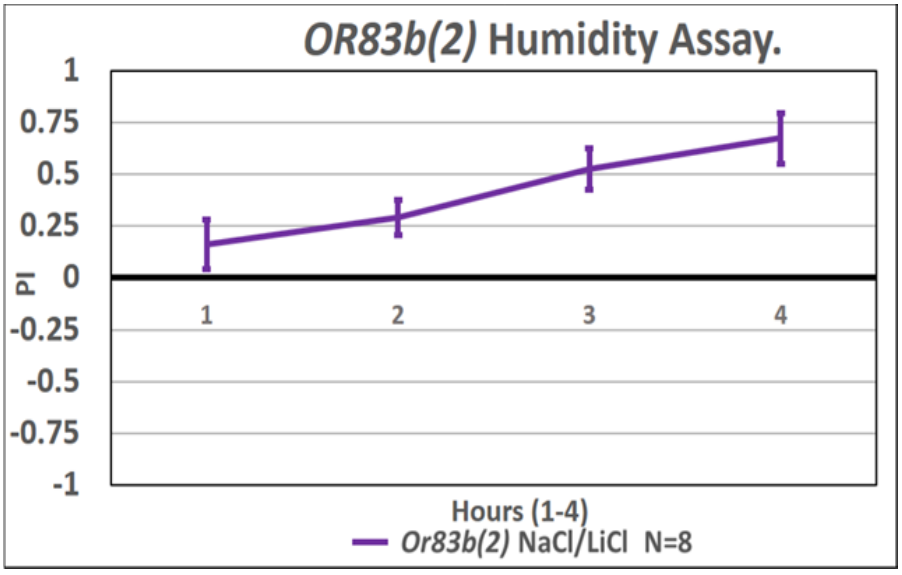

(C)

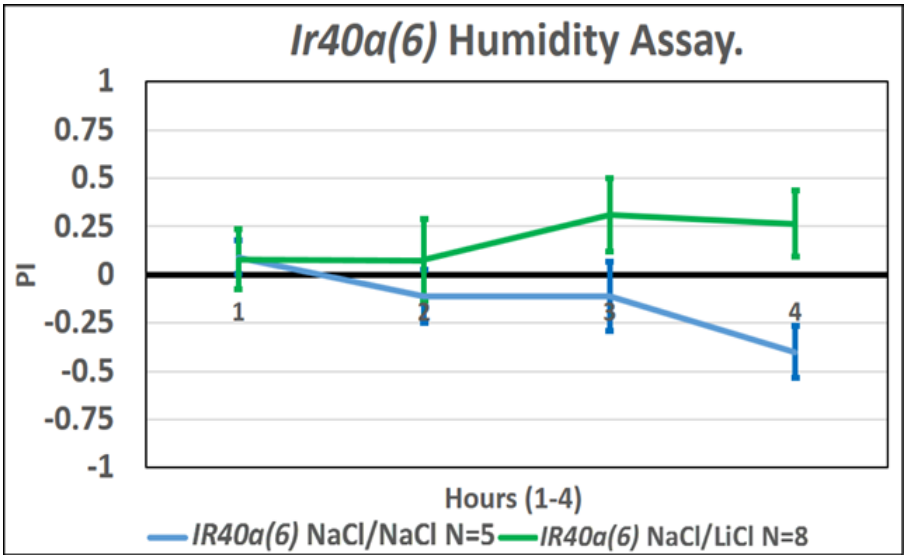
Ir40a(6) Humidity Assay.
1
0.75
0.5
0.25
0
-0.25
-0.5
-0.75
-1
PI
1
2
3
4
Hours (1-4)
IR40a(6) NaCl/NaCl N=5
IR40a(6) NaCl/LiCl N=8

(D)

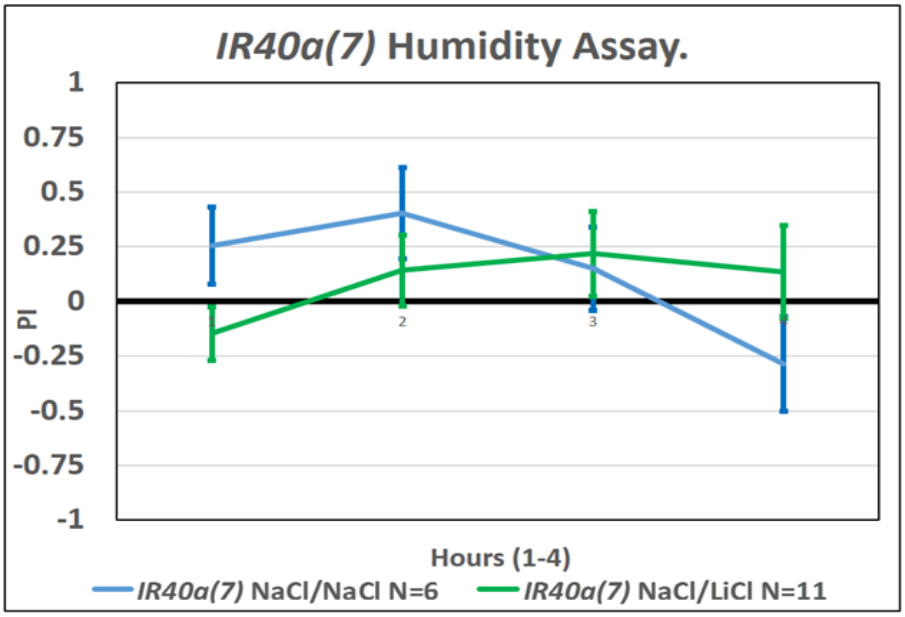
IR40a(7) Humidity Assay.
1
0.75
0.5
0.25
0
-0.25
-0.5
-0.75
-1
PI
2
3
Hours (1-4)
IR40a(7) NaCl/NaCl N=6
IR40a(7) NaCl/LiCl N=11

Figures 11

The CRISPR/Cas9 System

(A) Diagram of the CRISPR/Cas9 system and theory behind NHEJ and HDR. The CRISPR/Cas9 necessitates the Cas9 protein (transparent blue), a scaffold RNA (trRNA) (orange), PAM sequence (purple) and a crRNA (light blue) sequence that matches a genomic region (green). NHEJ is the result of a single cut (red) wherein nucleotides are randomly lost or gained (left). HDR occurs when two different cuts are made (red and purple). A nucleotide sequence can be inserted in HDR when a templet with arms matching the flanking genomic sequences is co-injected (right). (B) Breeding scheme of the CRISPR/Cas9 system used in *A. aegypti.*

(A)

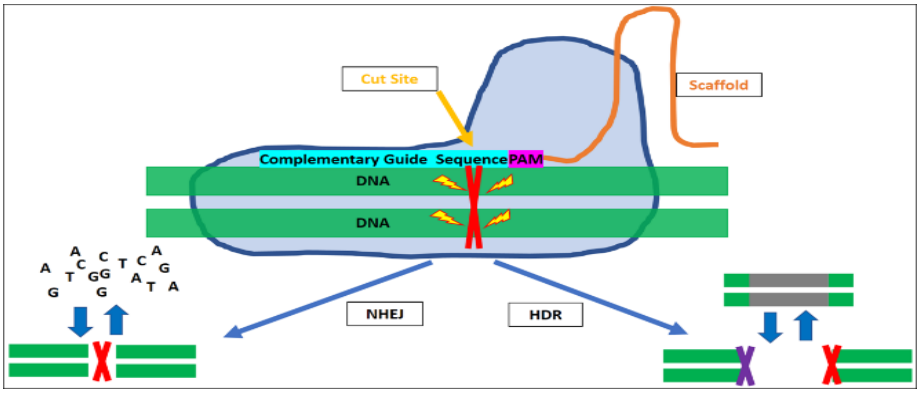

(B)

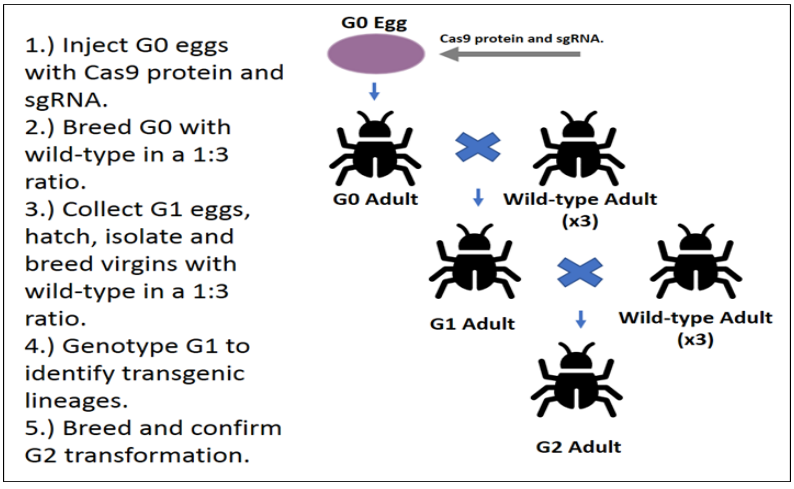

Figure 12

Egg Laying Chamber

Sufficient diH20 was added to oversaturate the filter paper and 5–10 *A. aegypti* females were transferred to these vials. The vials were put in a dark room to allow egg laying for 20-40 minutes.

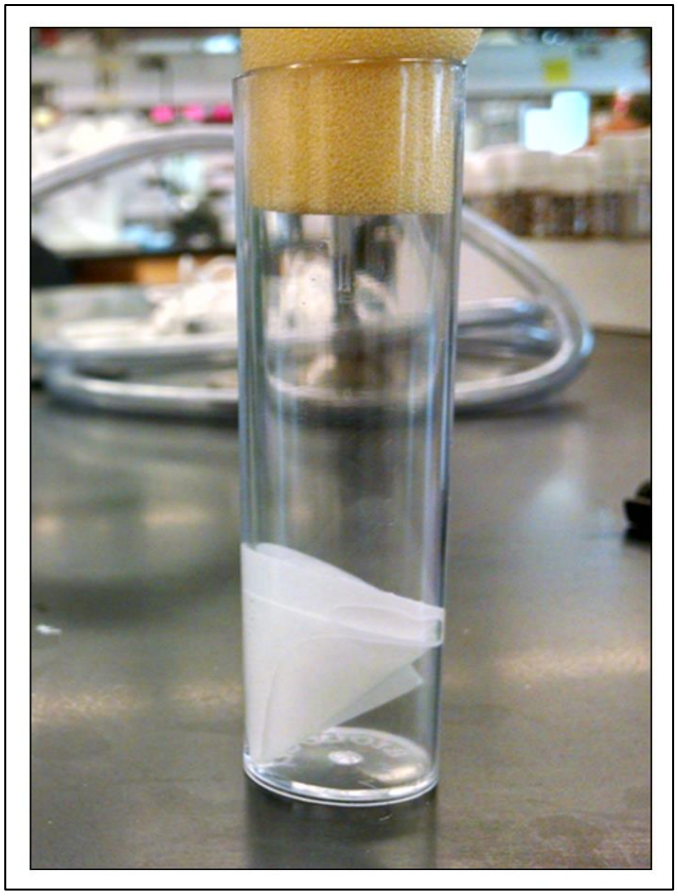

Figure 13

A. aegypti Egg Case Melanization and Microinjection Angle

(A) For the first attempts at creating IR40a and IR25a, light-purple melanized eggs (i) were injected ~40 minutes after being laid and 20 minutes of light exposure. For the subsequent attempts at IR40a and IR25a sgRNA injections, only light grey eggs (ii) were injected 20 minutes after being laid with 10–15 minutes of light exposure. Eggs that were exposed to light and air for too long developed a thicker egg case (iii). (B) Injection angle of *A. aegypti* eggs. Lines of *A. aegypti* eggs were stacked and injected with CRISPR/Cas. Following the first attempts of mutating IR40a and IR25a (left), eggs were injected at an ~20 degree angle (right).

(A)

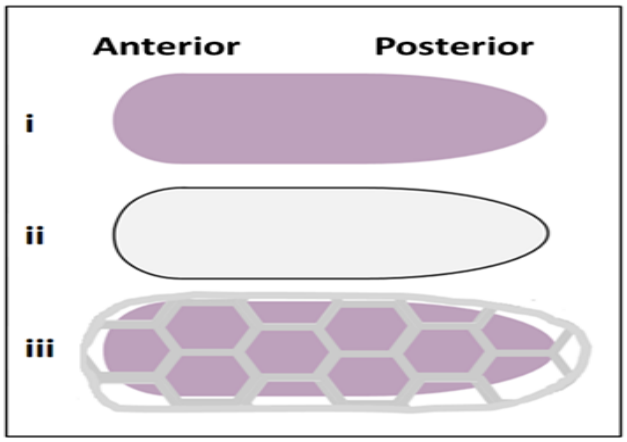

(B)

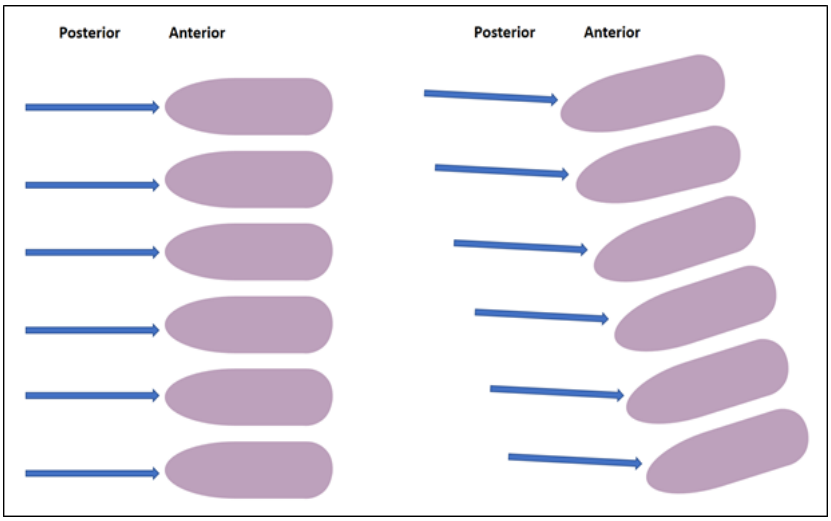

Figure 14

A. aegypti IR Genes of Interest

Illustration of IR genetic loci targeted by Maria Irigoyens' sgRNA and location of predicted cuts (blue arrows).

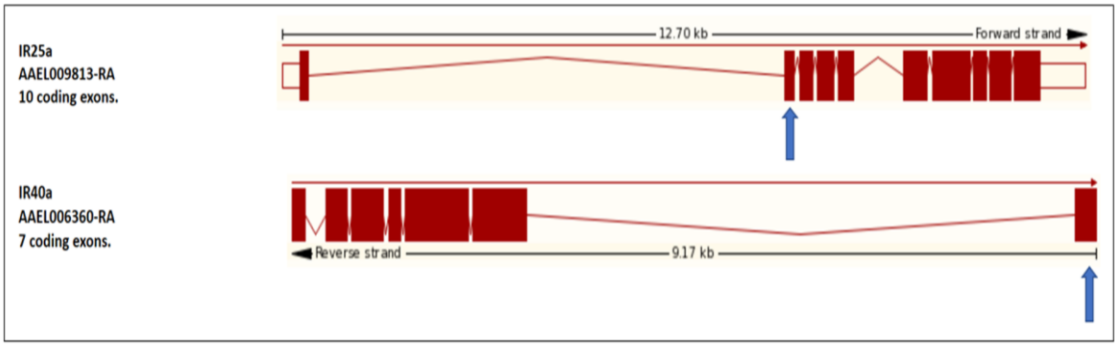

Figure 15

Diagnostic PCR Products and Cut Sites

PCR fragment sequences used for diagnostic PCR. PAM and restriction enzyme recognition sequences are highlighted in red and yellow respectively. Primers used are in Table 2. (A) IR40a and (B) IR25a.

(A)

Diagnostic restriction digest of *A. aegypti's* IR40a targeted INDEL site.

- 232 base pair PCR fragment. Cutting with StyI generates 203 and 29 base pair fragments.
- PAM, Sty1 cut site and sgRNA.

ATGAACAAAGTTCTTGCAACACCAGCTTCCAAGGCGGACAAGTTAGAGAGCCTTATCAGCATCG
GACTCGTGGTTCAAAATCTCTGCAGTCAGTTGCAGTCTATGAGAATGGAGGCCCATTTGTCCAA
CCCTTCTCTGCTGCAAGAACTGGTAGACAAGCTGCCAGCGAATATCAAGCTGCACTGGGCTTTG
CATCAACGACAAGTTCCAGTGGTGGATTTTCGCGCTTTCA

(B)

Diagnostic restriction digest of *A. aegypti's* IR25a targeted INDEL site.

- 232 base pair PCR fragment. Cutting with MnlI generates 203 and 29 base pair fragments.
- PAM, MnlI cut site and sgRNA.

TGTTTGTGAACGAAGTGGGTAATGATTTGGCGCAAGTTGCTGTAGATGTTGCGCTGAACTATAT
AAGAAAGAACCCAAGCCTCGGACTTTCAGTTGAGCTACTAACCGTCGAAGGAAACCGTACTGAC
AGCAAAGGGCTGTTGGAGTCGTGTAAGTATGAAAACAACACATATCTTCTGTATTGCGAGCTTC
GAAATTTATCATATTTTTCTCCCTTACGTCGCTTAATTAAGTGTGCTCAAAGTACACTGAAGCGAT
CAACACCAATCGGCCACCCCACGTAATATTTGACACTACTCTTACGGGCGTTTCTTCGGAAACGG
TGAAATCCATTAGTGCTGCGCTAGGAATTCCTACGGTTTCCGCATCAACCGGCCAAGAAGGCGA
CTT

Figure 16

Diagnostic Restriction Digest

Example diagnostic restriction digest results of IR40a G0s on 12/18/15. Lanes marked with asterisks indicate resistance to the Restriction Enzyme Mnl1 after a four-hour incubation and thus are indicated to contain transgenic tissue. Expected band size if no INDELs occurred are 29 and 203 base pairs. ThermoFisher GeneRuler 1 kb Plus DNA Ladder (Catalog# SM1331).

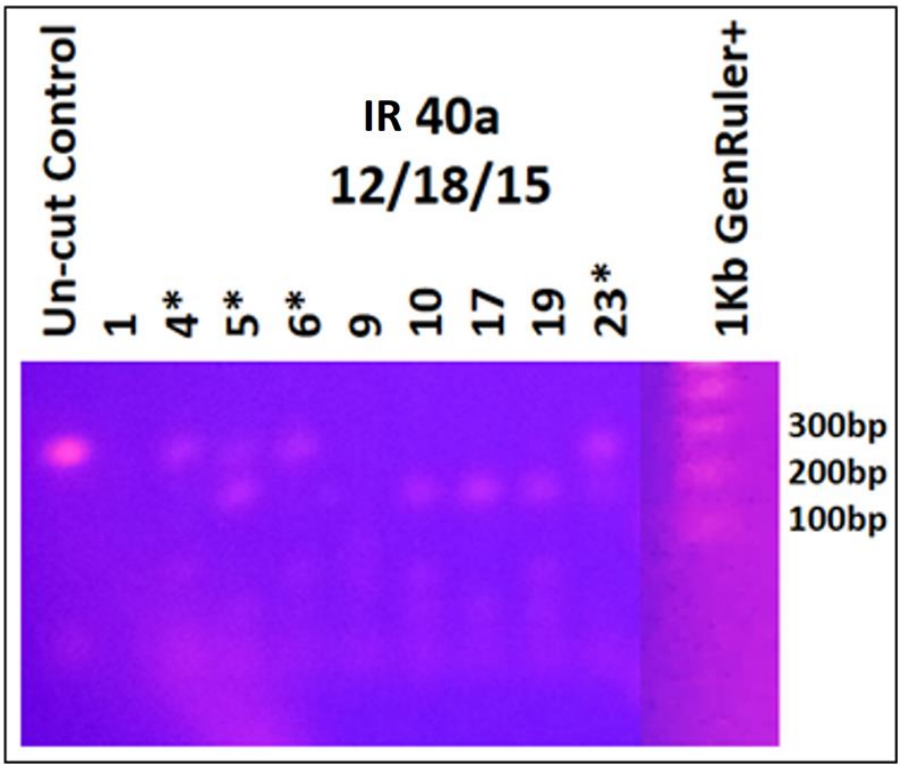

Figure 17

Retrogen Sequencing Results

Example results for IR25a candidate G1 specimen PCR products created using Accupure PCR MasterMix. Expected INDELs would occur at the middle of the “AGGCTT” sequence marked in red.

5/3/2016 Retrogen Sequence Results

~~>15~~-IR25a 376 61 294 0.05
NNNNNNNNNNNNNNNNNNTCTANNNNNNNNNNNNNTNGGNTTTGCNNNNNNTCCGAAGAAACGCCCGTAAG
AGTAGTGTCAAATATTACGTGGGGTGGCCGATTGGTGTTGATCGCTTCAGTGTACTTTGAGCACACTTAATTAAGC
GACGTAAGGGAGAAAAATATGATAAATTTCGAAGCTCGCAATACAGAAGATATGTGTTGTTTTCATACTTACACGA
CTCCAACAGCCCTTTGCTGTCAGTACGGTTTCCTTCGACGGTTAGTAGCTCAACTGAAAGTCCGAGGCTTGGGTTCT
TTCTTATATAGTTCAGCGCAACATCTACAGCAACTTGCGCCAAATCATTACCCACTTCGTTNNCAAACAGNNTNNN
N

~~>20~~-IR25a 377 57 298 0.05
NNNNNNNNNNNNNNNTNNNNNNNNNNNNNNNNNNNGNGNNNNCNCCGTNNNCCAGAAGAAACGCCCGTA
AGAGTAGTGTCAAATATTACGTGGGGTGGCCGATTGGTGTTGATCGCTTCAGTGTACTTTGAGCACACTTAATTAA
GCGACGTAAGGGAGAAAAATATGATAAATTTCGAAGCTCGCAATACAGAAGATATGTGTTGTTTTCATACTTACAC
GACTCCAACAGCCCTTTGCTGTCAGTACGGTTTCCTTCGACGGTTAGTAGCTCAACTGAAAGTCCGAGGCTTGGGT
TCTTTCTTATATAGTTCAGCGCAACATCTACAGCAACTTGCGCCAAATCATTACCCACTTCNNNNNACAAACNGNN
TANA

~~>25~~-IR25a 381 63 313 0.05
NNNNNNNNNNNNNNNNNNNNNNNNNNNGNNNCNNNANNNNGNTTTNCANCNNGTTTCCNAAGAAACGCC
CGTAAGAGTAGTGTCAAATATTACGTGGGGTGGCCGATTGGTGTTGATCGCTTCAGTGTACTTTGAGCACACTTAA
TTAAGCGACGTAAGGGAGAAAAATATGATAAATTTCGAAGCTCGCAATACAGAAGATATGTGTTGTTTTCATACTT
ACACGACTCCAACAGCCCTTTGCTGTCAGTACGGTTTCCTTCGACGGTTAGTAGCTCAACTGAAAGTCCGAGGCTT
GGGTTCTTTCTTATATAGTTCAGCGCAACATCTACAGCAACTTGCGCCAAATCATTACCCACTTCGTTCACAAACAG
GCTANAN

~~>26~~-IR25a 377 80 255 0.05
CNNNNNNNNNNNNNNNTNGNNNNNNNTNNNNNANNNGNNTTNGCCCGNNNNNNNATAANCGCCCGTAAG
AGTAGTGTCAAATATTACGTGGGGTGGCCGATTGGTGTTGATCGCTTCAGTGTACTTTGAGCACACTTAATTAAGC
GACGTAAGGGAGAAAAATATGATAAATTTCGAAGCTCGCAATACAGAAGATATGTGTTGTTTTCATACTTACACGA
CTCCAACAGCCCTTTGCTGTCAGTACGGTTTCCTTCGACGGTTAGTAGCTCAACTGAAAGTCCGAGGCTTGGGTTCT
TTCTTATATAGTTCAGCGCAACATCTACAGCAACTTGCGNCANATCCTTACCCACTTNNTNNNCAAAAAGANTNNN
NNN

~~>35~~-IR25a 373 77 272 0.05
NNNNNNNNNNNNNNNNNNCNNTCGNNNANNNNNNGNTANNANGTTNTANANNAGNTGCCCGTAAGAGTAGT
GTCAAATATTACGTGGGGTGGCCGATTGGTGTTGATCGCTTCAGTGTACTTTGAGCACACTTAATTAAGCGACGTA
AGGGAGAAAAATATGATAAATTTCGAAGCTCGCAATACAGAAGATATGTGTTGTTTTCATACTTACACGACTCCAA
CAGCCCTTTGCTGTCAGTACGGTTTCCTTCGACGGTTAGTAGCTCAACTGAAAGTCCGAGGCTTGGGTTCTTTCTTA
TATAGTTCTGCGCAACATCTACAGCAACTTGCGCCAAATCATTACCCACTTCNNTAACAAACANGNTAANNNNN

Table 1

Mean PI Values of *D. melanogaster* Humidity Gradient Assays

(A-C) W118 wild-type, *IR40a(6),* and *IR40a(7) D. melanogaster* flies were subjected to 70/70% NaCl/NaCl humidity gradients to serve as a two-choice experiment control. X's indicate time points where the room's lights turned off and data could not be collected.

(A) W118 70/70% RH gradient behavioral assay.

W118 NaCl/NaCl							
Date Time Video Plate	07/30/2016 8:00PM 1288 (1)	07/30/2016 8:00PM 1288 (2)	07/31/2016 3:41PM 1305 (1)	07/31/2016 3:41PM 1305 (2)	08/01/2016 9:10PM 1312 (1)	08/01/2016 9:10PM 1312 (2)	08/01/2016 9:10PM 1312 (3)
Hour 1	0.111111111	0.6	-0.090909091	-0.25	0.692307692	-0.555555556	0.166666667
Hour 2	0.333333333	0.6	0	-0.111111111	1	-0.333333333	0
Hour 3	0.090909091	0.272727273	-0.090909091	0.5	0.833333333	-0.555555556	-0.166666667
Hour 4	-0.142857143	0.272727273	-0.090909091	0.25	0.538461538	-0.5	0

(B) *IR40a(6)* 70/70% RH gradient behavioral assay.

IR40a(6) NaCl/NaCl					
Date Time Video Plate	07/30/2016 8:00PM 1288 (1)	07/30/2016 8:00PM 1288 (2)	07/31/2016 3:41PM 1305 (1)	07/31/2016 3:41PM 1305 (2)	08/01/2016 9:10PM 1312 (1)
Hour 1	-0.142857143	-0.090909091	0.333333333	-0.111111111	0.090909091
Hour 2	0	-0.6	0.230769231	-0.111111111	-0.111111111
Hour 3	0	-0.636363636	0.5	-0.111111111	-0.111111111
Hour 4	0	-0.6	0.076923077	0	-0.4

(C) *IR40a(7)* 70/70% RH gradient behavioral assay.

IR40a(7) NaCl/NaCl						
Date Time Video Plate	07/30/2016 8:00PM 1288 (1)	07/30/2016 8:00PM 1288 (2)	07/31/2016 3:41PM 1305 (1)	07/31/2016 3:41PM 1305 (2)	08/01/2016 9:10PM 1312 (1)	08/01/2016 9:10PM 1312 (2)
Hour 1	0	-0.666666667	-0.333333333	0.142857143	-0.090909091	0.6
Hour 2	0	-0.636363636	-0.454545455	0.428571429	0.090909091	0.714285714
Hour 3	0	-0.636363636	0.333333333	0.428571429	-0.272727273	0.571428571
Hour 4	0.2	-0.8	-0.076923077	0.384615385	-0.8	0.230769231

Table 2

Mean PI Values of *D. melanogaster* Humidity Gradient Assays

(A-D) W118 wild-type, *OR83b(2), IR40a(6),* and *IR40a(7) D. melanogaster* flies were subjected to 20/70% LiCl/NaCl humidity gradients to serve as a two-choice experiment. X's indicate time points where the room's lights turned off and data could not be collected.

(A) W118 20/70% RH gradient behavioral assay.

W118 LiCl/NaCl							
Date Time Video Plate	07/24/2016 5:12PM 1238 (1)	07/24/2016 5:12PM 1238 (2)	07/25/2016 11:24PM 1246 (1)	07/25/2016 11:24PM 1246 (2)	07/26/2016 6:30PM 1277 (1)	07/26/2016 6:30PM 1277 (2)	07/26/2016 6:30PM 1277 (3)
Hour 1	0.111111111	0	-0.4	0.166666667	0.5	0.4	0.090909091
Hour 2	-0.166666667	0.4	-0.2	-0.2	0.666666667	0.75	0.090909091
Hour 3	0.4	1	0.2	0.2	x	x	0.272727273
Hour 4	0.777777778	1	0.4	0.4	x	x	0.166666667

(B) *OR83b(2)* 20/70% RH gradient behavioral assay.

OR83b(2) LiCl/NaCl								
Date Time Video Plate	06/02/2016 1PM 1137 (1)	06/02/2016 1PM 1137 (2)	06/02/2016 1PM 1137 (3)	06/02/2016 1PM 1137 (4)	06/02/2016 1PM 1137 (5)	06/02/2016 1PM 1137 (6)	06/07/2016 4PM 1150 (1)	06/07/2016 4PM 1150 (2)
Hour 1	0.25	0.333333333	0.2	0.5	-0.25	0	-0.333333333	0.6
Hour 2	0.111111111	0.428571429	0	0.75	0.142857143	0.142857143	0.428571429	0.333333333
Hour 3	1	0.333333333	0.111111111	0.75	0.428571429	0.636363636	0.6	0.333333333
Hour 4	0.8	0.75	0.333333333	1	1	1	0.25	0.25

(C) *IR40a(6)* 20/70% RH gradient behavioral assay.

IR40a(6) LiCl/NaCl								
Date Time Video Plate	07/24/2016 5:12PM 1238 (1)	07/24/2016 5:12PM 1238 (2)	07/25/2016 11:24PM 1246 (1)	07/25/2016 11:24PM 1246 (2)	07/25/2016 1:57PM 1258 (1)	07/25/2016 1:57PM 1258 (2)	07/25/2016 8:45PM 1265 (1)	07/25/2016 8:45PM 1265 (2)
Hour 1	-0.5	-0.25	0.714285714	0.4	0.2	0.2	0.333333333	-0.454545455
Hour 2	-0.4	0.25	0.25	0.272727273	-1	1	0.428571429	-0.166666667
Hour 3	0	0.2	0.75	0.111111111	-0.2	1	x	x
Hour 4	-0.272727273	0.4	0.666666667	0	0	0.8	x	x

(D) *IR40a(7)* 20/70% RH gradient behavioral assay.

IR40a(7) LiCl/NaCl												
Date Time Video Plate	07/24/2016 5:12PM 1238 (1)	07/24/2016 5:12PM 1238 (2)	07/25/2016 11:24PM 1246 (1)	07/25/2016 11:24PM 1246 (2)	07/25/2016 1:57PM 1258 (1)	07/25/2016 1:57PM 1258 (2)	07/25/2016 8:45PM 1265 (1)	07/25/2016 8:45PM 1265 (2)	07/26/2016 6:30PM 1277 (1)	07/26/2016 6:30PM 1277 (2)	07/26/2016 6:30PM 1277 (3)
Hour 1	0.2	-0.2	0	0.555555556	-0.090909091	0.090909091	-0.5	-0.090909091	-0.777777778	0	-0.8
Hour 2	0.333333333	0.333333333	0.666666667	0.555555556	-0.166666667	0.5	-0.777777778	0.090909091	-0.777777778	0	0.8
Hour 3	0.714285714	0.4	0.666666667	0.555555556	0.454545455	0.4	x	x	-0.5	0.272727273	-1
Hour 4	0.8	0.6	0.428571429	0.333333333	0.454545455	0.6	x	x	-0.6	0.272727273	-1

Table 3

Targets of sgRNA

Genomic targets for CRISPR/Cas9 attempts in IR genes of *A. aegypti*. PAMs are in bold.

Target Gene	Target Genomic Sequence
IR25a	**CCC**AAGCCTCGGACTTTCAGTTG
IR40a	**CCA**GCTTCCAAGGCGGACAAGTT

Table 4

Diagnostic Restriction Digest Primers

Primers used to amplify sections of the indicated genes. PCR fragments were used for restriction digests (Figure 16).

Gene	Forward Primer	Reverse Primer
IR25a	5′ TGTTTGTGAACGAAGTGGGTAATG 3′	5′ AAGTCGCCTTCTTGGCCGGTTGATG 3′
IR40a	5′ ATGAACAAAGTTCTTGCAACAC 3′	5′ TGAAAGCGCGAAAATCCACCAC 3′

Table 5

Results of IR Targeting CRISPR/Cas9

Data summary of the use of the CRISPR/Cas9 system to target IR genes in *A. aegypti*. X's indicate that data was not collected.

Target gene (batch)	IR40a (Fall 2015)	IR25a (Winter 2015)	IR40a (Summer 2016)	IR25a (Fall 2016)
Adults/eggs injected.	78/734	63/622	82/721	12/91
Survival rate (%).	11%	10%	11.4%	13.2%
G0 restriction digest mutants identified.	18	16	X	X
G0 transformation rate (%).	23%	25%	X	X
G1 eggs raised.	22	52	64	49
Transgenic lineages established.	0	0	0	0